PHILOSOPHICAL TRANSACTIONS OF THE ROYAL SOCIETY A MATHEMATICAL, PHYSICAL & ENGINEERING SCIENCES

Null Field Approach to Scalar Diffraction. I. General Method

R. H. T. Bates and D. J. N. Wall

Phil. Trans. R. Soc. Lond. A 1977 **287**, 45-78
doi: 10.1098/rsta.1977.0139

Phil. Trans. R. Soc. Lond. A. **287**, 45–78 (1977) [45]
Printed in Great Britain

NULL FIELD APPROACH TO SCALAR DIFFRACTION
I. GENERAL METHOD

BY R. H. T. BATES† AND D. J. N. WALL‡
† *Electrical Engineering Department, University of Canterbury, Christchurch, New Zealand*
‡ *Mathematics Department, University of Dundee, Scotland DD1 4HN*

(*Communicated by D. S. Jones, F.R.S. – Received 27 August 1975 – Revised 26 January 1977*)

CONTENTS

Invoking the optical extinction theorem (extended boundary condition) the conventional singular integral equation (for the density of reradiating sources existing in the surface of a totally reflecting body scattering monochromatic waves) is transformed into infinite sets of non-singular integral equations, called the null field equations. There is a set corresponding to each separable coordinate system (we say that we are using the 'elliptic', 'spheroidal', etc., null field method when we employ 'elliptic cylindrical', 'spheroidal', etc., coordinates). Each set can be used to compute the scattering from bodies of arbitrary shape, but each set is most appropriate for particular types of body shape, as our computational results confirm. We assert that when the improvements (reported here) are incorporated into it, Waterman's adaptation of the extinction theorem becomes a globally efficient computational approach. Shafai's use of conformal transformation for automatically accomodating singularities of the surface source density is incorporated into the cylindrical null field methods. Our approach permits us to use multipole expansions in a computationally convenient manner, for arbitrary numbers of separated, interacting bodies of arbitrary shape. We present examples of computed surface source densities induced on pairs of elliptical and square cylinders.

1. General introduction

(*a*) *Preamble to the whole series of papers*

This is the first of a series of three papers treating, from a computational viewpoint, the diffraction of scalar waves by totally reflecting bodies. We use the 'null field method' which is our development of a technique based on what has been variously called the 'field equivalence principle', the 'optical extinction theorem' and the 'extended boundary condition'. We cover both direct and inverse scattering, illustrating our theoretical results with computational examples.

The direct scattering problem involves calculating the scattered field, given the field incident upon a body of known constitution and location. Solutions to this problem are straightforward in principle: they can be formulated without difficulty and programmed for a digital computer. However, as emphasized in two recent reviews (Jones 1974*b*; Bates 1975*b*), there is no shortage of computational pitfalls. We assert that, of the many available techniques, the null field method is perhaps the most promising because of two of its properties. First, the solutions are necessarily unique; the complementary problem (that of the cavity resonances internal to the scattering body) is automatically decoupled from the problem of interest (the exterior scattering problem) other methods have to be specially adapted to ensure this. The second property stems from the regularity of the kernels of the null field integral equations (the conventional integral equations have singular kernels); it is usually easy to expand the wave functions in terms of any desired basis functions, so that the latter can be chosen for computational, rather than analytical, convenience.

The calculation of multiple scattering by closely spaced bodies tends to be demanding of computer storage and time, which may account for the several iterative techniques which have been suggested. We show here that the null field method leads to efficient, direct computation of the simultaneous scattering from several cylinders of arbitrary cross-section.

Numerical algorithms based on exact solutions to direct scattering problems become computationally expensive if the dimensions of the scattering bodies are large compared with the wavelength, when it becomes appropriate to use approximate techniques such as the 'geometrical theory of diffraction' and 'physical optics'. Electrical engineers use the term 'physical optics' to describe the approximate techniques based on Kirchhoff's approach to diffraction: the reradiating sources induced at each point on the surface of a body are assumed to be identical to

those which would be induced, at the same point, on an infinite totally reflecting plane tangent to the point. We use the term 'planar physical optics' to describe this conventional Kirchhoff approach, because it is exact when the body is infinite and flat. In the second paper of this series we develop 'circular physical optics', 'elliptical physical optics', 'spherical physical optics', etc., which become exact when the body is a circular cylinder, elliptic cylinder, sphere, etc.

The inverse scattering problem involves calculating the shape of the body, given the incident field and the scattered field (most often it is the far scattered field that is given, i.e. the asymptotic, or Fraunhofer, form of the field). This is much more demanding computationally than the direct scattering problem, as is evinced by certain analytic continuation techniques which seem to be the only known, exact (in principle), general means of treating inverse scattering in two or three space dimensions. Approximate, computationally efficient methods based on asymptotic techniques, such as geometrical optics and planar physical optics, have been used with some success for certain simple scattering bodies. In the third paper of this series we develop from our extensions to physical optics a new approximate approach to inverse scattering which is of wider applicability than previous asymptotic approaches and is as convenient computationally.

(*b*) *Introduction to the present paper*

Up to the present, in the null field methods that are based on Waterman's (1965) formulation, the extended boundary condition is satisfied explicitly within the circle (for two-dimensional problems) or the sphere (for three-dimensional problems) inscribing the scattering body. Although such 'circular' and 'spherical' null field methods are theoretically sound, they tend to be unstable numerically when the body has a large aspect ratio. In this paper we generalize Waterman's formulation to satisfy the extended boundary condition explicitly within the ellipse (for two-dimensional problems) or the spheroid (for three-dimensional problems) inscribing the body, in order to ensure numerical convergence in situations where the circular and spherical null field methods lead to computational instabilities.

Ever since digital computers have been in general use, engineers and applied physicists have developed a multitude of heuristic methods for solving integral equations numerically. There has been a notable lack of critical, rigorous mathematical examinations of the methods, mainly because the pertinent mathematical results have not been easily accessible to non-mathematicians. But it seems that Zabreyko *et al.* (1975) have largely made good this deficiency in the literature; they have gathered together many diverse results and have covered points not properly considered before. The background to modern approaches to integral equations is covered rigorously, but most readably, by Pogorzelski (1966); concise treatments are given by Smithies (1958) and Green (1969). In this paper we place much reliance on Zabreyko *et al.* (1975), whose treatment is by far the most comprehensive we have yet seen.

Rayleigh (1892) is perhaps the first to have studied scattering from multiple bodies. He considered rectangular arrays of circular cylinders and spheres. Comprehensive surveys of the work which has followed are given by Twersky (1960), Burke & Twersky (1964) and Hessel & Oliner (1965).

Methods, which are in principle exact, are none too practicable for solving diffraction problems for bodies whose dimensions are large compared with the wavelength: the associated digital computations tend to be difficult to organize and are enormously expensive. Similarly, exact methods for solving multiple scattering problems are impracticable when the separations of the bodies are large, in which cases it has been shown that approximate methods can often provide

PHILOSOPHICAL TRANSACTIONS OF THE ROYAL SOCIETY A MATHEMATICAL, PHYSICAL & ENGINEERING SCIENCES

solutions of useful accuracy (Karp & Zitron 1961*a*, *b*; Twersky 1962*a*, *b*). When the bodies and separations are both small, low frequency approximations apply (Twersky 1962*a*, *b*, 1967). Exact solutions are most needed when the linear dimensions of the bodies and their spacings are of the order of the wavelength; this is fortunate because it means that useful digital computations can often be done efficiently.

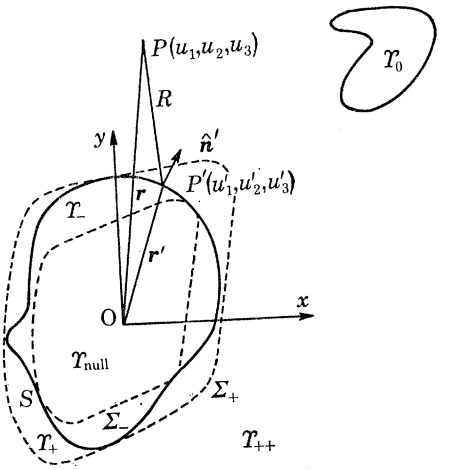

FIGURE 1. Cross-section of a three-dimensional scattering body showing a Cartesian coordinate system and a general orthogonal curvilinear coordinate system. In the Cartesian coordinate system the z-axis is perpendicular to, and directed out of the page.

In a scattering problem it is usually convenient to take the origin of coordinates inside the body. This implies that it is likely to be convenient to shift the origin during the solution of a multiple scattering problem. Such shifts can be accomplished with the aid of addition theorems, which exist for all wave functions which are solutions of the Helmholtz equation in separable coordinate systems (Morse & Feshbach 1953, Chs 10–13). The addition theorems have been applied to multiple bodies, on the surface of each of which one coordinate of a separable coordinate system (having its origin inside the body) has a constant value, i.e. each body is a spheroid, sphere, elliptic cylinder or circular cylinder. Direct solutions (cf. Row 1955; Liang & Lo 1967) of the equations so obtained have tended to require excessive computer time, so that iterative methods have been developed (Cheng 1969; Olaofe 1970), but these are often found to converge slowly (Cheng 1969). Howarth & Pavlasek (1973), Howarth (1973), Howarth, Pavalasek & Silvester (1974) and Ahluwalia & Boerner (1974) have recently developed numerically efficient techniques which are suitable for spherical and circularly cylindrical bodies. Peterson & Ström (1974) have extended Waterman's (1969*b*, 1971) approach to multiple scattering bodies whose shapes, while they cannot be arbitrary, need not be spherical or circularly cylindrical.

We employ addition theorems here, and our methods of solution are direct. Our improvement is that we can deal with multiple scattering bodies of arbitrary shape in a numerically efficient manner.

In § 2 necessary preliminaries are introduced. The optical extinction theorem is stated in § 3. Section 4 is devoted to the development of the general null field method, applicable to all separable coordinate systems. We emphasize that the shapes of the scattering bodies can be arbitrary. Particular null field methods are discussed in § 5. The concern in § 6 is with what has to be done to ensure computational efficiency. The null field treatment of multiple scattering bodies is

developed in § 7. In § 8 are presented computational results for the scattering of plane waves by cylindrical bodies having a variety of cross-sectional shapes. We assess in § 9 the significance of our results and suggest how they might be extended.

2. Preliminaries

As indicated in figure 1, three-dimensional space (denoted by $\mathcal{V}$) is partitioned according to

$$\mathcal{V} \sim \mathcal{V}_- \cup S \cup \mathcal{V}_+, \tag{2.1}$$

where $\mathcal{V}_-$ and $\mathcal{V}_+$, respectively, are the regions inside and outside the closed surface S of a totally reflecting body. Arbitrary points in $\mathcal{V}$ and on S are denoted by P and P′ respectively. With respect to the point O, which lies in $\mathcal{V}_-$, the position vectors of P and P′ are $\boldsymbol{r}$ and $\boldsymbol{r}'$ respectively.

The unit vector $\hat{\boldsymbol{n}}'$ is the outward normal to S at P′. Cartesian coordinates (x, y, z) and orthogonal curvilinear coordinates (u_1, u_2, u_3) are set up with O as origin; u_1 is a radial type of coordinate, u_2 is an angular type of coordinate, u_3 is either the same as z (for cylindrical coordinate systems) or is an angular type of coordinate (for non-cylindrical coordinate systems). The surface Σ_- and Σ_+, on which u_1 is constant, inscribe and circumscribe S in the sense that they are tangent to it but do not cut it. We define

$$\mathcal{V}_{\text{null}} \sim \text{region inside } \Sigma_-; \tag{2.2}$$

$$\mathcal{V}_{++} \sim \text{region outside } \Sigma_+. \tag{2.3}$$

Monochromatic (angular frequency ω, wavelength λ, wave number $k = 2\pi/\lambda$) impressed sources exist within the region $\mathcal{V}_0 \subset \mathcal{V}_{++}$. These sources radiate an incident field ψ_0, which impinges on the body inducing equivalent sources in S. The reradiations from these sources induce further sources, and so on until an equilibrium is reached. The totality of these sources gives rise to the scattered field ψ. All sources and fields are taken to be complex functions of space, with the time factor $\exp(\mathrm{i}\omega t)$ suppressed. There is no need to make a formal distinction between scattering and antenna problems, but it is worth remembering that $\mathcal{V}_0$ is usually far from $\mathcal{V}_-$ for the former and is always near to $\mathcal{V}_-$ for the latter.

We consider those fields whose propagation is governed by the Helmholtz equation:

$$\nabla^2\psi + k^2\psi = -f, \tag{2.4}$$

where f is the total surface density at P of the reradiating sources induced in S. The form of (2.4) implies that our results apply to all scalar fields which behave like acoustic fields of small amplitude.

In general, f varies from point to point on S, implying that f depends upon the parametric coordinates τ_1 and τ_2 introduced in table 1. We see then, on invoking a standard formulation of the diffraction of a scalar field by a material body (cf. Morse & Ingard 1968, § 7.1; Jones 1964, § 1.26), that the scattered field at P can be written as

$$\psi = \Lambda\left\{\int_S\int f g \,\mathrm{d}s\right\}, \quad f = f(\tau_1, \tau_2), \tag{2.5}$$

where Λ is the appropriate operator and g is the scalar free-space Green function:

$$g = g(kR) = \{\exp(-\mathrm{i}kR)\}/4\pi R, \tag{2.6}$$

where R is the distance from P′ to P: $\qquad R = |\boldsymbol{r} - \boldsymbol{r}'|.$ (2.7)

Totally reflecting bodies are either sound-soft or sound-hard. The forms of Λ and f in these two cases are

$$\Lambda = -1, \quad f = \lim_{\mathrm{P}\to\mathrm{P}'} \partial(\psi_0+\psi)/\partial n \quad \text{sound-soft}, \tag{2.8}$$

$$\Lambda = -\partial/\partial n, \quad f = \lim_{\mathrm{P}\to\mathrm{P}'} (\psi_0+\psi) \quad \text{sound-hard}, \tag{2.9}$$

where the n-direction is in the same sense as the n'-direction, but the operator $\partial/\partial n$ is applied to fields at P, whereas the operator $\partial/\partial n'$ is applied to fields at P′.

Like many who have gone before us we often find it useful and instructive to treat cylindrical scattering bodies, of infinite length but of arbitrary cross section. When $\partial f/\partial z \equiv 0$ all sources and fields are independent of z; and the explicit dimension of all quantities of interest decreases by one, when compared with the general case. It is sufficient to examine ψ within Ω, which is the infinite plane $z = 0$, and on C, which is the closed curve formed when Ω cuts S. In table 1 we compare quantities appropriate for scattering bodies of arbitrary shape and cylindrical scattering bodies; the table serves to *define* quantities not previously discussed in the text. We indicate the explicit functional dependence of fields and sources: note that we use C to denote both the curve and distance along it, measured anticlockwise from the outermost intersection of C with the x-axis.

TABLE 1. QUANTITIES APPROPRIATE FOR ARBITRARY SCATTERING BODIES AND CYLINDRICAL SCATTERING BODIES

(Note that not all circumflex accents introduced in this paper denote unit vectors, but only those which surmount symbols set in bold type.)

	arbitrary bodies	cylindrical bodies
regions of space	$\Upsilon, \Upsilon_0, \Upsilon_+, \Upsilon_{++}, \Upsilon_-, \Upsilon_{\mathrm{null}}$	$\Omega, \Omega_0, \Omega_+, \Omega_{++}, \Omega_-, \Omega_{\mathrm{null}}$
boundaries	S Σ_-, Σ_+	$C \sim S \cap \Omega$ Γ_-, Γ_+
coordinates	u_1, u_2, u_3 τ_1, τ_2 which are orthogonal parametric coordinates lying in S	u_1, u_2, z C
unit vectors	any vector symbol (bold type) surmounted by a circumflex accent e.g. $\hat{\boldsymbol{n}}, \hat{\boldsymbol{x}}$	
fields	$\psi = \psi(u_1, u_2, u_3)$	$\psi = \psi(u_1, u_2)$
source densities	$f = f(\tau_1, \tau_2)$	$F = F(C)$
Green functions	$\{\exp(-\mathrm{i}kR)\}/4\pi R$	$(-\mathrm{i}/4)\, H_0^{(2)}(kR)$ 'Hankel function of second kind of zero order'

There is an equivalent multipole expansion for g in each of the separable coordinate systems (cf. Morse & Feshbach 1953, Chs 7 and 11):

$$g = \sum_{l=0}^{\infty} \sum_{j=-l}^{l} c_{j,l} \hat{h}^{(2)}_{j,l}(u_1, k) \hat{\jmath}_{j,l}(u_1', k)\, \hat{Y}_{j,l}(u_2, u_3, k)\, \hat{Y}_{j,l}(u_2', u_3', k) \quad (u_1 \geqslant u_1'), \tag{2.10}$$

where the $c_{j,l}$ are normalizing constants and $\hat{h}^{(2)}_{j,l}(\cdot)$ and $\hat{\jmath}_{j,l}(\cdot)$ are those independent solutions, to the radial part of the scalar Helmholtz equation, corresponding respectively to waves which are outgoing at infinity and waves which are regular at the origin of coordinates. The radial solutions in the spherical coordinate system are independent of the subscript j (refer to § 5). The solutions $\hat{Y}_{j,l}(\cdot)$ are regular solutions of the part of the Helmholtz equation which remains after the radial part has been separated out. When $u_1' > u_1$, the argument of $\hat{h}^{(2)}_{j,l}$ becomes u_1', k and the

argument of $\hat{\jmath}_{j,l}$ becomes u_1, k. The way in which we have defined Υ_0 and ψ_0 ensures that the latter can be written as

$$\psi_0 = \sum_{l=0}^{\infty} \sum_{j=-l}^{l} c_{j,l} a_{j,l} \hat{\jmath}_{j,l}(u_1, k)\, \hat{Y}_{j,l}(u_2, u_3, k), \tag{2.11}$$

where the $a_{j,l}$ are appropriate expansion coefficients.

We denote a finite set of integers by

$$\{I_1 \to I_2\} \sim \{I_1, I+1, I_2+2, \ldots, I_2-1, I_2\}, \tag{2.12}$$

where I_1 and I_2 are integers, with $I_2 \geqslant I_1$. We define $\{I_2 \to I_1\}$ to be the null set unless $I_2 = I_1$.

(a) *Particular notation for cylindrical bodies*

When the scattering body is cylindrical and the fields exhibit no variation in the z-direction, only one angular coordinate enters into the functional dependence of the wave functions. So, the two integer-indices j and l can be replaced by a single one, m say. The wave functions are either even (denoted by the superscript e) or odd (denoted by the superscript o) about any suitable datum, which we choose to be the x-axis. Consequently, instead of $\hat{Y}_{j,l}(u_2, u_3, k)$ we have either $\hat{Y}^{\mathrm{e}}_m(u_2, k)$ or $\hat{Y}^{\mathrm{o}}_m(u_2, k)$. To accord more closely with conventional notation for wave functions appropriate to cylindrical coordinate systems, we replace $\hat{\jmath}_{j,l}$ and $\hat{h}^{(2)}_{j,l}$ by $\hat{J}_m$ and $\hat{H}^{(2)}_m$. When cylindrical polar coordinates are employed, $\hat{J}_m(u_1, k)$ and $\hat{H}^{(2)}_m(u_j, k)$ become the ordinary Bessel and Hankel functions $J_m(k\rho)$ and $H^{(2)}_m(k\rho)$ respectively. This is discussed in more detail in § 5 (*a*), but we point out here that there are distinct even and odd forms of the $\hat{J}_m$ and $\hat{H}^{(2)}_m$ for general cylindrical coordinate systems. The equations corresponding to (2.10) and (2.11) are

$$\begin{aligned} g = \sum_{m=0}^{\infty} [&c^{\mathrm{e}}_m \hat{H}^{(2)\mathrm{e}}_m(u_1, k)\, \hat{J}^{\mathrm{e}}_m(u_1', k)\, \hat{Y}^{\mathrm{e}}_m(u_2, k)\, \hat{Y}^{\mathrm{e}}_m(u_2', k) \\ &+ c^{\mathrm{o}}_m \hat{H}^{(2)\mathrm{o}}_m(u_1, k)\, \hat{J}^{\mathrm{o}}_m(u_1', k)\, \hat{Y}^{\mathrm{o}}_m(u_2, k)\, \hat{Y}^{\mathrm{o}}_m(u_2', k)] \quad (u_1 \geqslant u_1'); \end{aligned} \tag{2.13}$$

$$\psi_0 = \sum_{m=0}^{\infty} [c^{\mathrm{e}}_m a^{\mathrm{e}}_m \hat{J}^{\mathrm{e}}_m(u_1, k)\, \hat{Y}^{\mathrm{e}}_m(u_2, k) + c^{\mathrm{o}}_m a^{\mathrm{o}}_m \hat{J}^{\mathrm{o}}_m(u_1, k)\, \hat{Y}^{\mathrm{o}}_m(u_2, k)], \tag{2.14}$$

where the c_m are normalizing constants and the a_m are appropriate expansion coefficients. Throughout this paper we omit the superscripts e and o whenever it causes no ambiguity.

3. The extinction theorem

Given ψ_0 then either (2.8) or (2.9) can be combined with (2.5) to give a Fredholm integral equation for ψ on S. The Green function g is the kernel of the integral equation. Note that (2.10) is an expansion of g in a bilinear series of two sets of functions, the members of each set being orthogonal and square-integrable in three-dimensional space. However, the form of the expansion, at any point on S, depends upon the relative magnitudes of u_1 and u_1'. So, g cannot be expressed as a single bilinear series everywhere on S. Consequently, even though g has all the properties of a Fredholm kernel (cf. Zabreyko *et al.* 1975, Ch. I, § 1.1), the integral equation suffers from the well-known (cf. Jones 1974*a*, *b*) lack of uniqueness of its solution. For particular values of k (the so-called eigenvalues of the integral equation) the solution is contaminated by what correspond to resonances inside S.

The extinction theorem, which we now discuss, is based on the field inside S being explicitly zero. There cannot be any resonances, which means that the solutions to the integral equation are necessarily unique for all k.

When a body is totally reflecting, the incident and scattered fields are confined to Υ_+. Once f is known, ψ can be calculated from it using (2.5). This means that the actual material body need not be taken into account explicitly; it can be replaced by a 'disembodied' distribution of surface sources, identical in position and in complex amplitude with the actual surface sources. We can then think of ψ_0 as passing undisturbed throughout Υ and we can consider f to radiate into Υ_- as well as into Υ_+, so that (2.5) can be taken to apply throughout Υ. The optical extinction theorem states that

$$\psi = -\psi_0, \quad P \in \Upsilon_-. \tag{3.1}$$

It is physically obvious that a field cannot penetrate a totally reflecting body. But even when a body is partially opaque it is possible to define f such that the right-hand side (r.h.s.) of (2.5) 'extinguishes' ψ_0 in Υ_-, as seems to have been noticed first by Love (1901). Hönl, Maue & Westpfahl (1961) discuss the electromagnetic form of this principle. In the optical literature (cf. Born & Wolf 1970, § 2.4.2) the theorem is prefixed with the names Ewald (1916) and Oseen (1915).

On substituting (2.5) into (3.1) we obtain

$$-\psi_0 = \Lambda\left\{\int_S \int f g \, \mathrm{d}s\right\} \quad (P \in \Upsilon_-), \tag{3.2}$$

which we call the 'extended integral equation' for f, because Waterman (1965, 1969*a*, *b*, 1971, 1975) refers to the extinction theorem as the 'extended boundary condition'. Waterman can be excused for introducing new terminology because of the power of his approach. He expands g as in (2.10), using wave functions appropriate to spherical polar coordinates. This allows him to obtain from (3.2) an infinite set of non-singular integral equations which satisfy the extinction theorem explicitly within the inscribing sphere centred on the origin of coordinates. Avetisyan (1970), Hizal & Marincic (1970) and Bates & Wong (1974) have developed computational aspects of Waterman's approach, which has been extended in several significant particulars by Peterson & Ström (1974). However, the latter authors assume implicitly, as Waterman does, that the Rayleigh hypotheses (cf. Bates 1975*b*) are valid, and so their methods are less widely applicable (for totally reflecting bodies) than are those presented in this paper.

The two-dimensional analogue of Waterman's approach has been developed both for scattering problems (Bates 1968; Hunter 1972, 1974; Bolomey & Tabbara 1973; Bolomey & Wirgin 1974; Wirgin 1975) and for the computation of waveguide characteristics (Bates 1969; Ng & Bates 1972; Bates & Ng 1972, 1973).

Various methods have been developed in which the extinction theorem is satisfied either on surfaces, or at sets of points, arbitrarily chosen within Υ_- (Albert & Synge 1948; Synge 1948; Gavorun 1959, 1961; Vasil'ev 1959; Vasil'ev & Seregina 1963; Vasil'ev, Malushkov & Falunin 1967; Copley 1967; Schenck 1968; Fenlon 1969; Abeyaskere 1972; Taylor & Wilton 1972; Al-Badwaihy & Yen 1974). While these methods are useful for specific problems they do not have the generality of Waterman's approach, which satisfies the extinction theorem implicitly throughout Υ_- (this is discussed further in § 4). Al-Badwaihy & Yen (1975) have recently discussed the uniqueness of Waterman's approach and the aforementioned methods.

The null field method appears to provide added justification for the aperture-field method, an approximate design procedure useful in radio engineering (cf. Silver 1965, § 5.11), and for physical optics (Bates 1975*a*). It is amusing to note that the latter reference is among the first to remark that studies by acousticians and electrical engineers have run close on occasion to those of optical scientists, who have recently re-examined the extinction theorem in detail (Sein 1970, 1975; De Goede & Mazur 1972; Pattanayak & Wolf 1972).

4. The general null field method

We show here how to extend Waterman's approach by expanding g in wave functions appropriate to any separable coordinate system.

Consider the form of (3.2) for sound-soft bodies; (2.8) shows that $\Lambda = -1$. By definition, as laid down in (2.11), ψ_0 possesses an everywhere convergent expansion in terms of orthogonal functions, each of which is square-integrable. Now, r.h.s. (2.10) has a single form for $P \in \Upsilon_{\text{null}}$, because $u_1 \leqslant u_1'$ there. Consequently, g has a bilinear decomposition equivalent to (3.23) of Zabreyko *et al.* (1975). It follows from Zabreyko *et al.* (1975, Ch. III, § 6.2), given ψ_0, k and S, that there is a unique measurable f which is the solution to our (3.2).

When (2.9) is substituted into (3.2), the kernel becomes $\partial g/\partial n$ which, like g, is non-symmetric and possesses a single bilinear decomposition, valid $\forall P \in \Upsilon_{\text{null}}$, equivalent to (3.23) of Zabreyko *et al.* (1975).

We note that r.h.s. (2.5) and r.h.s. (3.2) are analytic throughout Υ_-, so that if f is chosen so that (3.2) is satisfied explicitly for all P within a finite part of Υ_- then, by elementary analytic continuation arguments (Waterman 1965; Bates 1968), (3.2) is necessarily satisfied implicitly for all P within Υ_-. In the spirit of Waterman, we manipulate (3.2) so as to satisfy it explicitly for all P within Υ_{null}, which is necessarily finite if the body has a finite interior. Consequently, we necessarily satisfy (3.2) implicitly for all P within Υ_-. Our method therefore has greater generality than alternative techniques (listed in § 3) in which the extinction theorem is satisfied explicitly only at points or on lines or on surfaces within Υ_-.

In an actual computation, (3.2) can only be satisfied approximately, even at points within Υ_{null}. In order that $|\psi + \psi_0|$ shall not exceed a required threshold, anywhere within Υ_-, we must compute f to a particular tolerance, which must be made smaller the larger Υ_- is in comparison with Υ_{null}. As Lewin (1970) forecast, numerical instabilities have tended to occur because of this, when Waterman's approach has been used to compute the scattering from bodies of large aspect ratio, and g has been expanded in wave functions appropriate to cylindrical or spherical polar coordinates (Bolomey & Tabbara 1973; Bolomey & Wirgin 1974; Bates & Wong 1974). We began the work reported in this paper when we realized that, by using elliptic cylinder coordinates or spheroidal coordinates, we could reduce the tendency towards numerical instability by decreasing the size of the part of Υ_- not included in Υ_{null}.

(a) *Sound-soft body*

On referring to the definition (2.2) of Υ_{null}, we see that (2.8), (2.13) and (2.14) permit (3.2) to be rewritten, since $u_1' > u_1$ in Υ_{null}, as

$$\sum_{l=0}^{\infty}\sum_{j=-l}^{l} c_{j,l}\hat{j}_{j,l}(u_1,k)\,\hat{Y}_{j,l}(u_2,u_3,k)\int_S\int f\hat{h}^{(2)}_{j,l}(u_1',k)\,\hat{Y}_{j,l}(u_2',u_3',k)\,\mathrm{d}s$$
$$= \sum_{l=0}^{\infty}\sum_{j=-l}^{l} c_{j,l}a_{j,l}\hat{j}_{j,l}(u_1,k)\,\hat{Y}_{j,l}(u_2,u_3,k) \quad P \in \Upsilon_{\text{null}}, \tag{4.1}$$

which is in the form that we have shown above to be equivalent to the integral equations treated in Zabreyko *et al.* (1975, Ch. III, § 6.2). So, we know there is a unique, measurable, square-integrable f that solves (4.1). The properties of the $\hat{Y}_{j,l}(\cdot)$ are such (cf. Morse & Feshbach 1953, Chs 7 and 11) that they form an orthogonal set on any closed surface $u_1 =$ constant. Since any

surface $u_1 =$ constant is closed with Υ_{null}, by definition, it follows that the individual terms in (4.1) are independent, so that

$$\int_S \int f \hat{h}^{(2)}_{j,l}(u_1', k)\, \hat{Y}_{j,l}(u_2', u_3', k)\, \mathrm{d}s = a_{j,l} \quad (l \in \{0 \to \infty\}, j \in \{-l \to l\}), \tag{4.2}$$

which are what we call the null field equations for a sound-soft body, for the particular separable coordinate system (u_1, u_2, u_3). The integrands are regular at all points on S because $\hat{h}^{(2)}_{j,l}(\cdot)$ is only singular on the surface $u_1' = 0$, which by definition cannot intersect S.

(b) *Sound-hard body*

It follows from (2.9) and (3.2) that

$$\psi_0 = \frac{\partial}{\partial n}\left(\int_S \int f g \, \mathrm{d}s\right), \quad P \in \Upsilon_-, \tag{4.3}$$

which can be rewritten, on account of the antisymmetry of g with respect to r and r', as

$$\psi_0 = -\int_S \int f (\partial g / \partial n')\, \mathrm{d}s \tag{4.4}$$

where we have noted the definition of $\partial/\partial n'$, relative to $\partial/\partial n$, given in § 2. Restricting P to lie within Υ_{null}, expressing g and ψ_0 in their multipole expansions (2.10) and (2.11) and again noting the orthogonality of the $\hat{Y}_{j,l}(\cdot)$ within Υ_{null}, we see that (4.4) leads to

$$\int_S \int f\, \partial(\hat{h}^{(2)}_{j,l}(u_1', k)\, \hat{Y}_{j,l}(u_2', u_3', k))/\partial n'\, \mathrm{d}s = -a_{j,l} \quad (l \in \{0 \to \infty\}, j \in \{-l \to l\}), \tag{4.5}$$

which are the null field equations for a sound-hard body, for the particular separable coordinate system (u_1, u_2, u_3).

(c) *Fields in* Υ_{++}

For $P \in \Upsilon_{++}$, we have $u_1 > u_1'$. It follows from substituting (2.10) into (2.5), and using (2.5) and (2.9), that

$$\psi = \sum_{l=0}^{\infty} \sum_{j=-l}^{l} c_{j,l} b_{j,l} \hat{h}^{(2)}_{j,l}(u_1, k)\, \hat{Y}_{j,l}(u_2, u_3, k), \quad P \in \Upsilon_{++}, \tag{4.6}$$

where

$$b_{j,l} = -\int_S \int f K^+_{j,l}\, \mathrm{d}s, \quad K^+_{j,l} = K^+_{j,l}(u_1', u_2', u_3', k), \tag{4.7}$$

where, for sound-soft bodies,

$$K^+_{j,l} = \hat{\jmath}_{j,l}(u_1', k)\, \hat{Y}_{j,l}(u_2', u_3', k) \tag{4.8}$$

and, for sound-hard bodies,

$$K^+_{j,l} = -\partial(\hat{\jmath}_{j,l}(u_1', k)\, \hat{Y}_{j,l}(u_2', u_3', k))/\partial n'. \tag{4.9}$$

(d) *Far fields*

Once f has been determined, by solution of the null field equations, the far scattered field can be conveniently computed from (2.5), with g assuming its asymptotic form: i.e. R is taken as the mean value of r.h.s. (2.7) in the denominator of r.h.s. (2.6), but R is approximated by

$$R = |\boldsymbol{r}| - \boldsymbol{r}' \cdot \boldsymbol{r}/|\boldsymbol{r}| \tag{4.10}$$

in the exponent in r.h.s. (2.6). The partial wave expansion of the far scattered field is obtained by expressing the $\hat{h}^{(2)}_{j,l}(\cdot)$ in (4.6) in their asymptotic forms (cf. Morse & Feshbach 1953, Chs 5, 10–12).

5. Particular null field methods

The coordinates u_1, u_2 and u_3 must belong to one of those sets for which the scalar Helmholtz (wave) equation separates (cf. Morse & Feshbach 1953, pp. 655–664). We say that (4.2) and (4.5) are the sound-soft and sound-hard equations for the 'spherical' null field method when u_1, u_2 and u_3 are specialized to the spherical polar coordinates r, θ and ϕ. Table 2 lists, for the spherical null field method, the forms assumed by the wavefunctions and the normalization constants $c_{j,l}$. Corresponding forms, appropriate to spheroidal and ellipsoidal coordinates, are given by Morse & Feshbach (1953, Chs 5, 10, 11), Meixner & Schäfke (1954) and Flammer (1957).

Table 2. Quantities appropriate for the spherical null field method

general null field method	spherical null field method
u_1, u_2, u_3	r, θ, ϕ
$\hat{\jmath}_{j,l}(u_1, k)$	$\hat{\jmath}_l(kr)$, spherical Bessel function of order l
$\hat{h}^{(2)}_{j,l}(u_1, k)$	$h^{(2)}_l(kr)$, spherical Hankel function of order l
$\hat{Y}_{j,l}(u_2, u_3, k)$	$P^j_l(\cos\theta)\exp(ij\phi)$, where $P^j_l(\cdot)$ is an associated Legendre function
$c_{j,l}$	$(-ik/4\pi)(2l+1)(l-j)!/(l+j)!$

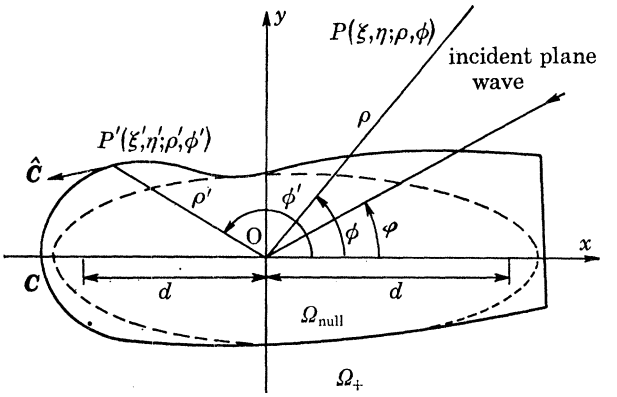

Figure 2. Cross-section of arbitrary cylindrical body and associated coordinate systems. The z-axis is perpendicular to, and directed out of the paper.

(a) *Cylindrical null field methods*

When treating cylindrical bodies of arbitrary cross section it is appropriate to make use of the notation introduced in table 1 and the cylindrical coordinates and wave functions discussed in § 2 (*a*). There are two cylindrical null field methods: the 'circular' for which u_1 and u_2 are the cylindrical polar coordinates ρ and ϕ, and 'elliptic' for which u_1 and u_2 are the elliptic cylinder coordinates ξ and η. Figure 2 depicts the cross section of an arbitrary cylindrical body. Cylindrical polar coordinates are indicated explicitly, while elliptic cylinder coordinates are indicated implicitly. Note that $2d$ is the separation of the foci of the elliptic cylinder coordinates. Table 3 lists the forms assumed by the wave functions and the normalization constants for the circular and elliptic null field methods.

We find it convenient to write both the even and odd null field equations in the form

$$\int_C F(C)\, K_m^-(C)\, \mathrm{d}C = a_m \quad (m \in \{0 \to \infty\}), \tag{5.1}$$

where the forms of $K_m^{-\mathrm{e}}(C)$ and $K_m^{-\mathrm{o}}(C)$ are listed in table 4, for the circular and elliptic null field methods.

Reasoning similar to that presented in § 3 (*c*) shows that, for points in Ω_{++}, it is permissible to write

$$\psi = \sum_{m=0}^{\infty} [c_m^{\mathrm{e}} b_m^{\mathrm{e}} \hat{H}_m^{(2)\mathrm{e}}(u_1, k)\, \hat{Y}_m^{\mathrm{e}}(u_2, k) + c_m^{\mathrm{o}} b_m^{\mathrm{o}} \hat{H}_m^{(2)\mathrm{o}}(u_1, k)\, \hat{Y}_m^{\mathrm{o}}(u_2, k)], \quad P \in \Omega_{++}, \tag{5.2}$$

where both the even and odd b_m can be expressed as

$$b_m = \int_C F(C)\, K_m^{+}(C)\, \mathrm{d}C \quad (m \in \{0 \to \infty\}). \tag{5.3}$$

We list c_m^{e}, c_m^{o}, $K_m^{+\mathrm{e}}(C)$ and $K_m^{+\mathrm{o}}(C)$ for the circular and elliptic null field methods in tables 3 and 4.

TABLE 3. WAVE FUNCTIONS APPROPRIATE FOR CYLINDRICAL NULL FIELD METHODS

null field method	$\hat{J}_m^{\times}(u_1, k)$	$\hat{H}_m^{(2)\times}(u_1, k)$	$\hat{Y}_m^{\times}(u_2, k)$	$c_m^{\times}$
circular	$J_m(k\rho)$ Bessel function of first kind of order m	$H_m^{(2)}(k\rho)$ Hankel function of second kind of order m	$\cos(m\phi)$, $\times = \mathrm{e}$ $\sin(m\phi)$, $\times = \mathrm{o}$	$-i/2$, $m > 0$ $-i/4$, $m = 0$
elliptic	$R_{\times m}^{(1)}(kd, \xi)$ modified Mathieu function of first kind, even and odd, of order m	$R_{\times m}^{(4)}(kd, \xi)$ modified Mathieu function of fourth kind, even and odd, of order m	$S_{\times m}(kd, \eta)$ Mathieu function even and odd, of order m	$-i/I_m^{\times}$

d = semi-focal distance of elliptic cylinder coordinate system. Refer to Morse & Feshbach (1953, Ch. 11).

$$I_m^{\times} = \int_{-1}^{1} S_{\times m}^2(kd, \eta)\, (1-\eta^2)^{-\frac{1}{2}}\, \mathrm{d}\eta;$$

$\times$ denotes either e (even) or o (odd).

TABLE 4. KERNEL FUNCTIONS APPROPRIATE FOR CYLINDRICAL NULL FIELD METHODS

(Refer to table 3 for definitions of notation.)

null field method	$K_m^{-\times}(C)$
circular (sound-soft)	$-H_m^{(2)}(k\rho') \begin{matrix}\cos\\ \sin\end{matrix} (m\phi')$
circular (sound-hard)	$\frac{1}{2}k \left[H_{m+1}^{(2)}(k\rho') \begin{matrix}\sin\\ \cos\end{matrix} \{(m+1)\,\phi' - \zeta_1'\} + H_{m-1}^{(2)}(k\rho') \begin{matrix}\sin\\ \cos\end{matrix} \{(m-1)\,\phi' + \zeta_1'\} \right]$
elliptic (sound-soft)	$-R_{\times m}^{(4)}(kd, \xi')\, S_{\times m}(kd, \eta')$
elliptic (sound-hard)	$(1/kd)\,(\xi'^2 - \eta'^2)^{-\frac{1}{2}} [(\xi'^2-1)^{\frac{1}{2}} \cos(\zeta_2' - \zeta_1')\, S_{\times m}(kd, \eta')\, (\mathrm{d}/\mathrm{d}\xi')\, R_{\times m}^{(4)}(k, \xi') - (1-\eta'^2)^{\frac{1}{2}} \sin(\zeta_2' - \zeta_1')\, R_{\times m}^{(4)}(kd, \xi')\, (\mathrm{d}/\mathrm{d}\eta')\, S_{\times m}(kd, \eta')]$

The formulas for $K_m^{+\times}(C)$ differ from those for $K_m^{-\times}(C)$ only in that J_m replaces $H_m^{(2)}$ and $R_{\times m}^{(1)}$ replaces $R_{\times m}^{(4)}$.

The angles ζ_1 and ζ_2 are defined by

$$\cos\zeta_1 = -\hat{\boldsymbol{C}}\cdot\hat{\boldsymbol{x}}; \qquad \sin\zeta_1 = -\hat{\boldsymbol{z}}\cdot(\hat{\boldsymbol{x}}\times\hat{\boldsymbol{C}});$$
$$\cos\zeta_2 = \boldsymbol{\eta}\cdot\hat{\boldsymbol{x}}; \qquad \sin\zeta_2 = \hat{\boldsymbol{z}}\cdot(\hat{\boldsymbol{x}}\times\boldsymbol{\eta}).$$

6. NUMERICAL CONSIDERATIONS

The numerical solution of the null field equations can be accomplished by adapting standard moment methods (cf. Harrington 1968). But there are several subtle points which are not encountered with the conventional integral equations. They vary slightly for sound-soft and

sound-hard bodies and for the several null field methods. But the important aspects are common to all null field equations. In this section the detailed argument is confined to sound-soft bodies, in order to simplify the symbolism as much as possible. We comment on sound-hard bodies when they involve noticeably different considerations.

(*a*) *General considerations*

Define $K^{-}_{j,l}$ to be the factor multiplying f in the integrand of (4.2). Consider the functions, $\tilde{\Psi}_{j,l}$ say, which are biorthogonal to the $K^{-}_{j,l}$ over S, in the sense defined by Pogorzelski (1966, Ch. VII, § 4). The form of (4.2) is such that $\tilde{f}_L$, where

$$\tilde{f}_L = \sum_{l=0}^{L} \sum_{j=-l}^{l} a_{j,l} \tilde{\Psi}_{j,l}, \tag{6.1}$$

must converge to f, in a mean-square sense, as $L \to \infty$. The Gram–Schmidt orthonormalization procedure (cf. Morse & Feshbach, 1953, pp. 928–931; Pogorzelski 1966, Ch. IV, § 1; Zabreyko *et al.* 1975, Ch. III, § 1) can also be invoked to derive (6.1). Waterman (1969*b*, 1971) has examined analytical and numerical aspects of this.

It is convenient to define

$$\bar{e}_L = \int_S \int |f - \bar{f}_L|^2 \, \mathrm{d}s, \tag{6.2}$$

where the superbar can stand either for a tilde (as in the two previous paragraphs) or for a circumflex accent (see the next paragraph). We also need to set a mean square tolerance, e_a say, which is acceptable for an approximate numerical evaluation of f. This tolerance has to be gauged according to criteria determined by whatever physical situation is being investigated.

Numerical solutions to integral equations are usually protracted and they can be expensive. Except in trivial cases where the $\tilde{\Psi}_{j,l}$ turn out to be directly proportional to the complex conjugates of the $K^{-}_{j,l}$ (i.e. when u'_1 is constant over S) the required number of computational operations is proportional to L^3 (cf. Harrington 1968). So, our main concern is with reducing L, or, equivalently, M (see § 6 (*b*) below), even at the expense of mathematical rigour. In fact, we have learnt to avoid approximating f by r.h.s. (6.1), although its ultimate convergence is established, because we know by example that r.h.s. (6.1) can be computationally awkward (Bates & Wong 1974; Bates 1975*b*). Our computational experience persuades us that there usually exist functions, $\hat{\Psi}_{j,l}$ say, independent over S but not biorthogonal to the $K^{-}_{j,l}$, and expansion coefficients, $\alpha_{j,l}$ say, such that $\hat{f}_L$, where

$$\hat{f}_L = \sum_{l=0}^{L} \sum_{j=-l}^{l} \alpha_{j,l} \hat{\Psi}_{j,l}, \tag{6.3}$$

converges more rapidly to f than does $\tilde{f}_L$. By this we mean that the least value of L, for which $\hat{e}_L < e_a$, is significantly less than the least value of L for which $\tilde{e}_L < e_a$.

As Jones (1974*b*) has emphasized, there do not seem to exist any methods for estimating *a priori* how large L must be to ensure that $\bar{e}_L < e_a$. The best that can be done is to choose a particular L, say L', and then compute $\bar{e}_{L'}$, $\bar{e}_{L'+1}$, $\bar{e}_{L'+2}$, etc., and continue until numerical convergence is (apparently) manifest.

Experience shows that the value of L, for which $\hat{e}_L < e_a$, is usually least when the $\hat{\Psi}_{j,l}$ accord with the required physical behaviour of f (cf. Bates 1975*b*). When S is an analytic surface, the $\hat{\Psi}_{j,l}$ should be analytic also. If there are points and/or lines on S, at or on which S ceases to be analytic, the $\hat{\Psi}_{j,l}$ should exhibit the appropriate singular behaviour in neighbourhoods of the

non-analytic parts of S (namely the edge conditions, which must be satisfied by electromagnetic fields (Jones 1964, § 9.2)). Even when S is analytic, it is not ideal to represent f by basis functions whose mean effect is the same everywhere – i.e. functions such as $\exp(\mathrm{i}[\gamma_1\tau_1+\gamma_2\tau_2])$, where γ_1 and γ_2 are real constants. There does not appear to be any way of handling this explicitly, for a scattering body of arbitrary shape. But there does exist a suitable method for a cylindrical scattering body, for which the surface S reduces to the boundary curve C, and the three-dimensional space Υ reduces to the two-dimensional space Ω (refer to table 1). We discuss this in detail in § 6 (*b*) below, which is devoted to cylindrical scattering bodies: these have been studied in greater computational depth than bodies of arbitrary shape because they involve much less computational effort and expense.

(*b*) *Considerations for cylindrical bodies*

In practice we can only solve a finite simultaneous number, $2M+1$ say, of the null field equations (5.1). If we restrict the integer m to the set $\{0 \to M\}$ then we cannot usefully employ more than $2M+1$ independent basis functions in a representation of $F(C)$. Note that when $m=0$ the odd basis function necessarily vanishes, which is why we have $2M+1$ and not $2M+2$ independent functions. By analogy with (6.3) we write

$$F_M = F_M(C) = \sigma(C)\sum_{m=0}^{M}[\alpha_m^{\mathrm{e}}\Psi_m^{\mathrm{e}}(C)+\alpha_m^{\mathrm{o}}\Psi_m^{\mathrm{o}}(C)], \tag{6.4}$$

where the α_m are expansion coefficients, the Ψ_m are appropriate basis functions and the superscripts e and o denote 'even' and 'odd', as in §§ 2 (*a*) and 5 (*a*). We include a weighting function $\sigma = \sigma(C)$ for later convenience. There is no need to repeat or amplify any of the discussion relating to $\tilde{f}_L$ and $\hat{f}_L$, so we do not need to affix a tilde or circumflex accent to F_M or Ψ_m.

In the neighbourhood of any point on C where C ceases to be analytic, $F = F(C)$ can be expressed in the form

$$F = \nu\omega, \tag{6.5}$$

where ω is analytic and ν is either integrably infinite or is singular in its nth order, and higher, derivatives (the value of n characterizes the type of singularity of F). Some, at least, of the Ψ_m should exhibit the same singular behaviour in the neighbourhood of the singular point on C. The computational advantage of using such singular functions has been demonstrated by Hunter & Bates (1972) and Hunter (1972, 1974) who deal with several singularities (simultaneously present on the surfaces of cylindrical bodies) by dividing the surfaces of the bodies into contiguous sections, on each of which F is approximated by a series of the form of (6.4).

Variations in curvature of C affect the mutual interaction between the surface sources existing in C, thereby causing concentrations and dilutions of $F(C)$ which increase the error sensitivity of numerical solutions to the null field equations. Since a circle exhibits no changes of curvature, the possibility of transforming C into a circle is worth investigating. Consider the conformal transformation of Ω_+ on to the exterior of a unit circle, an arbitrary point on which is identified by the angle ϑ. The element of arc $\mathrm{d}C$ and the differential angular increment around the circle are related by

$$\mathrm{d}C = h\,\mathrm{d}\vartheta, \tag{6.6}$$

where h is the metric coefficient characterizing the 'geometric irregularity' of C. If C is analytic then so is h, but the latter exhibits integrable singularities at values of ϑ corresponding to any points where C ceases to be analytic. Table 5 lists the metric coefficients which we use in various computational examples presented in this series of papers. Bickley (1929, 1934) gives larger lists,

based on the exterior form of the Schwarz–Christoffel transformation (cf. Morse & Feshbach 1953, § 4.7). General shapes can be transformed using formulas given by Kantorovich & Krylov (1958, Ch. 5).

Shafai (1970) shows that, if h is considered as a function of C rather than of ϑ, it satisfies

$$h = 1/\nu \tag{6.7}$$

at each singularity (if there is one or more) of C, for sound-soft bodies. This suggests that the factor σ introduced in (6.4) should be written as

$$\sigma = 1/h \tag{6.8}$$

because, when (6.4) and (6.6) are substituted into (5.1), in the sound-soft body case, the metric coefficient h cancels out.

TABLE 5. METRIC COEFFICIENT $h(\vartheta)$ OBTAINED BY TRANSFORMATION OF THE REGION Ω_+ FOR A SQUARE, RECTANGLE, EQUILATERAL TRIANGLE AND ELLIPSE ON TO THE EXTERIOR OF THE UNIT CIRCLE

cross-sectional shape	$h(\vartheta)$	transformation constants
square	$a\{\cos(2\vartheta)\}^{\frac{1}{2}}/E$	$E = 0.847$ a = half length of a side
rectangle	$a(m-\sin^2\vartheta)^{\frac{1}{2}}/E$	a = half length of longest side b = half length of shortest side For $b/a = 0.1$, $m = 0.1055$, $E = 0.840$ Refer to Bickley (1934) for other b/a ratios
equilateral triangle	$a\{\cos(\frac{2}{3}\vartheta)\}^{\frac{3}{2}}/E$	$E = 1.186$ a = half length of a side
ellipse	$(a^2\sin^2\vartheta + b^2\cos^2\vartheta)^{\frac{1}{2}}$	a = semi-major axis b = semi-minor axis

For sound-hard bodies no convenient cancellation of the metric coefficient is possible because there is no simple formula such as (6.7) connecting h and ν. However, F is always finite at singularities of C. It is usually most convenient to set $\sigma = 1$ in (6.4) and use Ψ_m which are regular everywhere on C, but it is advisable to make the substitution (6.6) in the null field equations so that the factor h can compensate, at least partially, for variations in the curvature of C; this is what we do for the applications presented in § 8. However, it is worth remembering that numerical instabilities can occur in the neighbourhoods of singularities of C, so that it is sometimes preferable to forgo the substitution (6.6) and instead use the Ψ_m which exhibit the appropriate singular behaviour. There is no precise algorithm for deciding *a priori* which is the more profitable procedure.

In conventional integral equation formulations of scattering problems, the kernels are usually singular, and it is often inconvenient to use other than the simplest basis functions – pulse-like functions, or even delta functions – so that one solves the integral equations by the method of subsections (Harrington 1968). The matrix orders required to determine F to within a desired tolerance are found to be much larger than for the null field methods.

(c) *Specific computational considerations*

All the computational results which we present in § 8 are for cylindrical scattering bodies.

Substituting (6.4) into both the even and odd forms of (5.1) gives (using × to denote either e or o)

$$\sum_{q=0}^{M} [\alpha_q^{\mathrm{e}} \Phi_{m,q}^{\mathrm{e}\times} + \alpha_q^{\mathrm{o}} \Phi_{m,q}^{\mathrm{o}\times}] = -a_m^{\times} \quad (m \in \{0 \to M\}), \tag{6.9}$$

where the four $\Phi_{m,q}^{\times\times}$ are defined by

$$\Phi_{m,q}^{\times\times'} = \int_C \sigma(C)\, \Psi_q^{\times}(C)\, K_m^{-\times'}(C)\, \mathrm{d}C. \tag{6.10}$$

When we use the transformation (6.6), we always take the $\Psi_q(C)$ to be

$$\Psi_q^{\mathrm{e}}(C) = \cos(q\vartheta) \quad \text{and} \quad \Psi_q^{\mathrm{o}}(C) = \sin(q\vartheta). \tag{6.11}$$

The $\Phi_{m,q}$ are the elements of the matrix that must be inverted to obtain the α_m from the a_m. We define the norm (denoted by Z) of this matrix to be the determinant of the $Z_{p,q}$ where

$$Z_{p,q} = \Phi_{p,q} \Big/ \left(\sum_{m=0}^{M} |\Phi_{m,q}|^2 \right)^{\frac{1}{2}}. \tag{6.12}$$

We have previously found this norm to be useful (Bates & Wong 1974) and Conte (1965, Ch. 5) shows that it is a good measure for comparing the relative condition of different matrices. We tabulate the order of Z, i.e. $O(Z)$. The smaller Z is, the greater is the error in the computed inverse matrix, for a given round-off error in individual arithmetic operations.

The computer time needed to perform a calculation is perhaps the most important factor which must be taken into account when attempting to assess a particular numerical technique. Unfortunately, there are such great differences between the many existing computing systems that bare statements of central processing unit (c.p.u.) times are not too meaningful. However, we feel that it should become accepted practice to record c.p.u. times, if only to give an 'order-of-magnitude' idea of the amount of computation involved. We list pertinent c.p.u. times in the captions to several of our tables and figures. For our computations we used the Boroughs B6718 digital computer (48-bit word) at the Computer Centre of the University of Canterbury. We used the extended Simpson rule (Abramowitz & Stegun 1968, formula 25.4.6) for all numerical evaluation of integrals. As our integrands are oscillatory there seems to be little point in attempting to use higher quadrature formulae (cf. Ng & Bates 1972). We used Blanch's (1964, 1966) rapid and accurate algorithms for computing Bessel and Mathieu functions.

As we point out in § 6 (*a*) there is no alternative at present to the brute-force procedure for checking whether numerical convergence is occurring. For a particular M we note the values of C (denoted by C_0, C_1 and C_2 respectively) for which $|F_M(C)|$, $|F_M^{(1)}(C)|$ and $|F_M^{(2)}(C)|$ are largest, where

$$F_M^{(n)}(C) = F_{M-n}(C) - F_M(C) \quad (n \in \{1, 2\}). \tag{6.13}$$

We say (arbitrarily) that the computation of $F(C)$ has converged (numerically) when

$$|F_M^{(n)}(C_n)/F_M(C_0)| < 0.03 \tag{6.14}$$

for n equal to both 1 and 2.

We take the incident field ψ_0 to be a plane wave incident at the angle φ. The appropriate expansion coefficients a_m for the series r.h.s. (2.14) are listed in table 6. All the bodies that we

examine are symmetric about $\phi = 0$, which means that the even–odd and odd–even matrix elements, introduced in (6.9) and (6.10), are automatically zero:

$$\Phi^{eo}_{q,m} = \Phi^{oe}_{q,m} = 0 \quad (q, m \in \{0 \to M\}). \tag{6.15}$$

This significantly reduces the amount of computation required to obtain values of f and ψ to a particular, desired accuracy. In fact, it reduces from $2M+1$ to $M+1$ the order of the matrix that must be inverted.

TABLE 6. COEFFICIENTS IN PLANE WAVE EXPANSIONS FOR CYLINDRICAL NULL FIELD METHODS

(Refer to table 3 for definitions of elliptic cylinder (Mathieu) functions.)

null field method	a^e_m	a^o_m
circular	$4\mathrm{i}^{m+1}\cos(m\phi)$	$4\mathrm{i}^{m+1}\sin(m\phi)$
elliptic	$\sqrt{8}\,\mathrm{i}^{m+1}S_{em}(kd, \cos\phi)$	$\sqrt{8}\,\mathrm{i}^{m+1}S_{om}(kd, \cos\phi)$

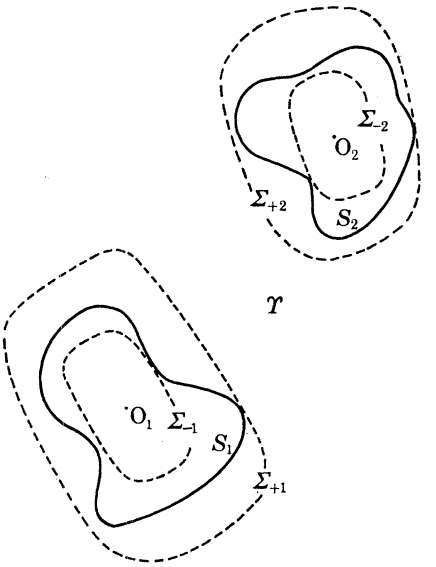

FIGURE 3. A pair of separated scattering bodies.

7. NULL FIELD TREATMENT OF MULTIPLE SCATTERING BODIES

Figure 3 shows a pair of totally reflecting bodies embedded in the space Ψ. The surfaces of both bodies are closed. In keeping with the notation introduced in § 2, we partition Υ according to

$$\Upsilon \sim \Upsilon_{-1} \cup S_1 \cup \Upsilon_{+1}; \quad \Upsilon \sim \Upsilon_{-2} \cup S_2 \cup \Upsilon_{+2}, \tag{7.1}$$

where S_1 is the surface of the first body and Υ_{-1} and Υ_{+1} are, respectively, the parts of space inside and outside S_1. The point $O_1 \subset \Upsilon_{-1}$ is taken as origin for an orthogonal curvilinear coordinate system (u_{11}, u_{21}, u_{31}). The surfaces Σ_{-1} and Σ_{+1}, on each of which the radial-type coordinate u_{11} is constant, respectively inscribe and circumscribe S_1, in the sense that they are tangent to it but do not cut it. We define

$$\Upsilon_{\mathrm{null}\,(1)} \sim \text{region inside } \Sigma_{-1}; \tag{7.2}$$

$$\Upsilon_{+1} \sim \text{region outside } \Sigma_{+1}. \tag{7.3}$$

The notation for the second body is similar. We define

$$\hat{\Upsilon}_{++} \sim \Upsilon_{++1} \cap \Upsilon_{++2}. \tag{7.4}$$

A monochromatic field ψ_0, originating from sources existing entirely within $\hat{\Upsilon}_{++}$, impinges upon the bodies inducing equivalent sources in their surfaces. Referring to (2.5) and employing an obvious extension of notation, we see that we can write the scattered field ψ as

$$\psi = \psi_1 + \psi_2, \quad P \in \Upsilon_{+1} \cap \Upsilon_{+2}; \tag{7.5}$$

$$\psi_1 = A\left\{\int_{S_1} f_1 g \, \mathrm{d}s\right\} \tag{7.6}$$

where f_1 is the density of equivalent surface sources induced in S_1; f_2 is written similarly. We find it convenient to introduce the terminology: 'the exterior and interior multipole expansions of ψ_1' by which we mean the expansions, valid for $P \in \Upsilon_{++1}$ and $P \in \Upsilon_{\mathrm{null}(1)}$ respectively, of r.h.s. (7.6) got by expanding g as in (2.10).

The first essential step in our approach is, by analogy with § 3, to replace the material bodies by 'disembodied' distributions of surface sources, identical in position and in complex amplitude with f_1 and f_2. Then ψ can be written as

$$\psi = \psi_1 + \psi_2, \quad P \in \Upsilon, \tag{7.7}$$

with ψ_1 given by (7.6), and ψ_2 expressed similarly. We then apply the optical extinction theorem to the two bodies separately:

$$\psi = -\psi_0, \quad P \in \Upsilon_{-1}; \tag{7.8}$$

$$\psi = -\psi_0, \quad P \in \Upsilon_{-2}, \tag{7.9}$$

which lead to simultaneous sets of extended integral equations, by analogy with (3.2), for f_1 and f_2.

Since the bodies are separated, $\Upsilon_{-1} \cap \Upsilon_{-2}$ is necessarily empty. However, in certain cases Σ_{-1} intersects Σ_{+2} and/or Σ_{-2} intersects Σ_{+1}. We define $\hat{\Sigma}_{-1}$ to be the largest closed surface, on which u_{11} is constant, contained within $\Upsilon_{\mathrm{null}(1)}$ and not intersecting Σ_{+2}. We define $\hat{\Upsilon}_{\mathrm{null}(1)}$ to be the region of space inside $\hat{\Sigma}_{-1}$. We see that $\hat{\Upsilon}_{\mathrm{null}(1)} \sim \Upsilon_{\mathrm{null}(1)}$ when Σ_{+2} does not intersect Σ_{-1}. We define $\hat{\Upsilon}_{\mathrm{null}(2)}$ similarly.

We obtain null field equations, analogous to (4.2) and (4.5), in the following way. By analogy with § 4 we satisfy (7.8) explicitly for $P \in \hat{\Upsilon}_{\mathrm{null}(1)}$; the analytic continuation arguments quoted in § 4 then ensure that (7.8) is satisfied throughout Υ_{-1}, provided that $\hat{\Upsilon}_{\mathrm{null}(1)}$ is not infinitesimal. In the latter case the null field method can still be applied if the exterior multipole expansion of ψ_2 converges within a finite part of $\Upsilon_{\mathrm{null}(1)}$ containing O_1. This is the same as requiring that the singularities of the exterior multipole expansion of ψ_2 lie within a surface, on which u_{12} is constant and is less than the value u_{12} has at O_1 (refer to Bates's 1975 *b* discussion of the Rayleigh hypothesis and related matters). We expand g in multipoles and proceed exactly as in § 4 to develop the interior multipole expansion of ψ_1. We re-express ψ_2 as a function of the coordinates u_{11}, u_{21}, u_{31}, instead of the coordinates u_{12}, u_{22}, u_{32}, using the appropriate addition theorem (Zaviska 1913; Stein 1961; Saermark 1959; Sack 1964; Cruzan 1962; King & Van Buren 1973). We then find that ψ_2 can be expanded, within $\hat{\Upsilon}_{\mathrm{null}(1)}$, in the same sort of interior multipole expansion as ψ_1. after handling (7.9) similarly, we have sufficient null field equations to give ψ_1 and ψ_2 uniquely – we develop the formalism in § 7 (*a*) below.

When we have N bodies ($N > 2$) we use the subscripts p and t, attached to the same symbols

as we have employed above, to identify quantities associated with individual bodies. We again constrain the sources of ψ_0 to lie within $\hat{\Upsilon}_{++}$, which we now define by

$$\hat{\Upsilon}_{++} = \bigcap_{t=1}^{N} \Upsilon_{++t}. \tag{7.10}$$

We satisfy the extinction theorem separately within each body. For the pth body we satisfy the theorem explicitly within $\hat{\Upsilon}_{\mathrm{null}(p)} \subset \Upsilon_{\mathrm{null}(p)}$, where $\hat{\Upsilon}_{\mathrm{null}(p)}$ is the part of space inside the closed surface $\hat{\Sigma}_{-p}$, which is yet to be defined. We define $\hat{\Sigma}_{+t}$, $t \in \{1 \to N\}$, to be the smallest closed surface on which u_{1t} is constant and which encloses all the singularities of the exterior multipole expansion of ψ_t. If any of the $\hat{\Sigma}_{+t}$, $t \neq p$, enclose O_p, for any $p \in \{1 \to N\}$, then the method introduced in this paper fails. When none of the $\hat{\Sigma}_{+t}$ enclose O_p, we define $\hat{\hat{\Sigma}}_{+p}$ to be that member of $\{\hat{\Sigma}_{+t};\ t \in \{1 \to p-1\} \cup \{p+1 \to N\}\}$ which approaches closest to O_p. If $\hat{\hat{\Sigma}}_{+p}$ does not intersect Σ_{-p} then we may say that $\hat{\Sigma}_{-p} \sim \Sigma_{-p}$. If $\hat{\hat{\Sigma}}_{+p}$ does intersect Σ_{-p} then we define $\hat{\Sigma}_{-p}$ to be that surface on which u_{1p} is constant and which is tangent to $\hat{\hat{\Sigma}}_{+p}$ but does not cut it.

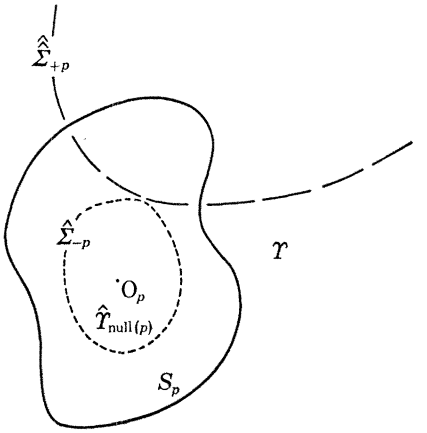

FIGURE 4. The pth scattering body.

It is worth realizing that in the majority of situations of interest none of the Σ_{+t} will intersect each other, let alone enclose any of the O_p. Since $\hat{\Sigma}_{+t}$ cannot enclose Σ_{+t}, because the latter must enclose all the singularities of the exterior expansion of ψ_t (cf. Bates 1975*b*) it follows that usually $\hat{\Sigma}_{-p} \sim \Sigma_{-p}$ for all $p \in \{1 \to N\}$. However, we include the previous paragraph for completeness.

We expand ψ_p within $\hat{\Upsilon}_{\mathrm{null}(p)}$ in its interior multipole expansion. We expand all other ψ_t within $\hat{\Upsilon}_{\mathrm{null}(p)}$ in a similar multipole expansion by applying the appropriate addition theorems to their exterior multiple expansions. Repeating this procedure for all $p \in \{1 \to N\}$ we obtain sufficient null field equations to give all members of $\{f_t;\ t \in \{1 \to N\}\}$ uniquely.

(*a*) *Null field formalism for multiple bodies*

Figure 4 shows the pth of a number of separated, interacting scattering bodies. We now give precise symbolic expression to the argument developed above. Our notation is an obvious extension of that introduced in § 2; but note the superscripts + and − affixed to the symbol b to identify exterior and interior multipole expansions respectively.

The j, lth term of the interior multipole expansion of ψ_p is

$$c_{j,l}\, b^{-}_{j,l,p}\, \hat{j}_{j,l}(u_{1p}, k)\, \hat{Y}_{j,l}(u_{2p}, u_{3p}, k), \tag{7.11}$$

where

$$b^{-}_{j,l,p} = \int_{S_p} \int f_p(\tau_{1p}, \tau_{2p})\, K^{-}_{j,l}(\tau_{1p}, \tau_{2p})\, \mathrm{d}s. \tag{7.12}$$

The j, lth term of the exterior multipole expansion of ψ_t is

$$c_{j,l} b^{+}_{j,l,t} \hat{h}^{(2)}_{j,l}(u_{1t}, k)\, \hat{Y}_{j,l}(u_{2t}, u_{3t}, k), \tag{7.13}$$

where $t \neq p$ and

$$b^{+}_{j,l,t} = \int_{S_t}\int f_t(\tau_{1t}, \tau_{2t})\, K^{+}_{j,l}(\tau_{1t}, \tau_{2t})\, \mathrm{ds}. \tag{7.14}$$

Use of the appropriate addition theorem (see references quoted in § 2) allows (7.13) to be rewritten as

$$c_{j,l} b^{+}_{j,l,t} \sum_{l'=0}^{\infty} \sum_{j'=-l'}^{l'} A_{t,p,j,j',l,l'} \hat{j}_{j',l'}(u_{1p}, k)\, \hat{Y}_{j',l'}(u_{2p}, u_{3p}, k) \tag{7.15}$$

within $\hat{\Upsilon}_{\mathrm{null}(p)}$, where

$$A_{t,p,j,j',l,l'} = \sum_{l''=0}^{\infty} \sum_{j''=-l''}^{l''} \alpha_{j,j',j'',l,l',l''} \hat{h}^{(2)}_{j'',l''}(u_{1tp}, k)\, \hat{Y}_{j'',l''}(u_{2tp}, u_{3tp}, k), \tag{7.16}$$

where the $\alpha_{j,j',j'',l,l',l''}$ depend upon the particular addition theorem being invoked and $(u_{1tp}, u_{2tp}, u_{3tp})$ are the coordinates of O_p in the tth coordinate system.

We choose an arbitrary point O within Υ as origin for a further system of coordinates identified by $t = 0$. We use (2.11) to represent the incident field ψ_0, but with u_1, u_2 and u_3 replaced by u_{10}, u_{20} and u_{30} respectively. The aforementioned addition theorems allow ψ_0 to be represented similarly within $\hat{\Upsilon}_{\mathrm{null}(p)}$, but in terms of wave functions depending upon u_{1p}, u_{2p} and u_{3p}. We add a further subscript p to the $a_{j,l}$ to identify the latter representation. We find that

$$a_{j,l,p} = \frac{1}{c_{j,l}} \sum_{l'=0}^{\infty} \sum_{j'=-l'}^{l'} c_{j',l'} a_{j',l'} A_{0,p,j',j,l',l}. \tag{7.17}$$

We note that $\{\hat{Y}_{j,l}(u_{2p}, u_{3p}, k);\, l \in \{0 \to \infty\}, j \in \{-l \to l\}\}$ is a set of functions orthogonal on any surface which is contained within $\hat{\Upsilon}_{\mathrm{null}(p)}$ and on which u_{1p} is constant. The extinction theorem, applied to the fields within $\hat{\Upsilon}_{\mathrm{null}(p)}$, then ensures that

$$b^{-}_{j,l,p} + \frac{1}{c_{j,l}} \sum_{l=0}^{N(p)} \sum_{l'=0}^{N} \sum_{j'=-l'}^{l'} c_{j',l'} b^{+}_{j',l',t} A_{t,p,j',j,l',l} = -a_{j,l,p} \quad (l \in \{0 \to \infty\}, j \in \{-l \to l\}), \tag{7.18}$$

where the superscript (p) on the summation sign indicates that the term for $t = p$ is missing. There is a set of equations (7.18) for all $p \in \{1 \to N\}$.

(*b*) *Circular null field method for two bodies*

The formulae needed for the applications presented in § 8 (*c*) are listed here. We restrict ourselves to a pair of bodies and we use only the circular null field method (figure 5).

If $\mathscr{Z}_m(\cdot)$ denotes any Bessel function of order m, the addition theorem (cf. Watson 1966, Ch. 11) gives

$$\mathscr{Z}_m(k\rho_t)\, \mathrm{sc}\,(m\phi_t) = \frac{1}{\epsilon_m} \sum_{n=0}^{\infty} \epsilon_n [A^{\times}_{t,p,m,n}\, \mathrm{sc}\,(n\phi_p) + B^{\times}_{t,p,m,n}\, \mathrm{sc}\,(n\phi_p)]\, J_n(k\rho_p) \quad (m \in \{0 \to \infty\}) \tag{7.19}$$

provided that $\rho_p < \rho_{12}$, where $t, p \in \{1, 2\}$ and $p \neq t$ and

$$\begin{aligned} A^{\times}_{t,p,m,n} &= (-1)^{m-n} A^{\times}_{p,t,m,n} \\ &= \tfrac{1}{2}\epsilon_m [\mathscr{Z}_{m-n}(k\rho_{tp}) \cos\{(m-n)\,\phi_{tp}\} \pm (-1)^n \mathscr{Z}_{m+n}(k\rho_{tp}) \cos\{(m+n)\,\phi_{tp}\}] \end{aligned} \tag{7.20}$$

and

$$\begin{aligned} B^{\times}_{t,p,m,n} &= (-1)^{m-n} B^{\times}_{p,t,m,n} \\ &= \tfrac{1}{2}\epsilon_m [\pm \mathscr{Z}_{m-n}(k\rho_{tp}) \sin((m-n)\,\phi_{tp}) + (-1)^n \mathscr{Z}_{m+n}(k\rho_{tp}) \sin\{(m+n)\,\phi_{tp}\}], \end{aligned} \tag{7.21}$$

where the Neumann factor ϵ_n is 1 for $n = 0$ and 2 for $n > 0$; and where sc $(\cdot)$ denotes cos $(\cdot)$ and the upper sign in $\pm$ is taken when $\times$ denotes e, but sc $(\cdot)$ denotes sin $(\cdot)$ and the lower sign in $\pm$ is taken when $\times$ denotes o. In (7.19) the bar surmounting $\times$ denotes that $\bar{\times}$ is o when $\times$ is e, and vice versa. This notation is used throughout the remainder of this section.

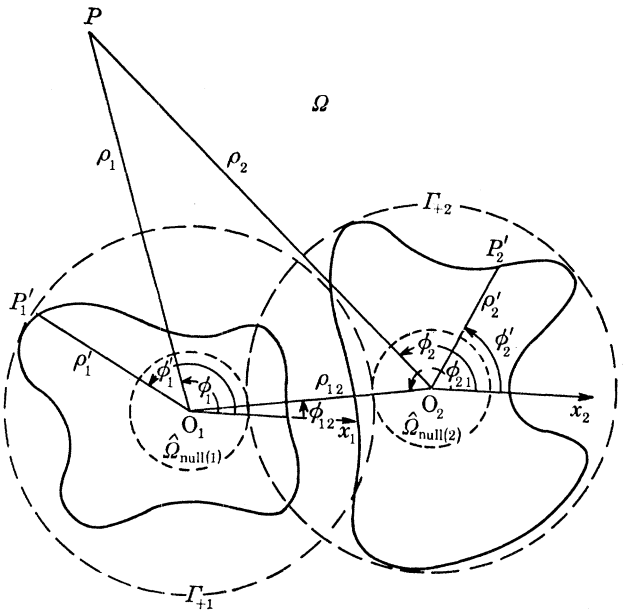

FIGURE 5. Cross-sectional geometry of scatterers.

We present formulae suitable for digital computation. Instead of referring the multipole expansion of the incident field to an arbitrary point $O \in \Omega$ as origin, in conformity with the general treatment presented in § 6 (*a*) above, we start with ψ_0 referred to O_1 as origin:

$$\psi_0 = (-i/4) \sum_{n=0}^{M_1} \epsilon_m [a^{e}_{m,1} \cos(m\phi_1) + a^{o}_{m,1} \sin(m\phi_1)] J_m(k\rho_1), \tag{7.22}$$

where the $a_{m,1}$ are given. The addition theorem (7.19) then shows that the expansion coefficients of the representation for ψ_0 referred to O_2 as origin are

$$a^{\times}_{m,2} = \sum_{n=0}^{M_1} [a^{\times}_{n,1} A^{\times}_{1,2,m,n} + a^{\bar{\times}}_{n,1} B^{\times}_{1,2,n,m}] \quad (m \in \{0 \to M_2\}), \tag{7.23}$$

where $\mathscr{Z}$ is replaced by J in r.h.s. (7.20) and r.h.s. (7.21), which means that the constraint $\rho_2 < \rho_{12}$ no longer applies (cf. Watson 1966, § 11.3). In general, M_1 and M_2 need to be different if the surface source densities on both bodies are to be computed to the same accuracy.

In conformity with the notation introduced earlier we write the expansion coefficients of the interior and exterior multipole expansions of ψ_t, $t \in \{1 \to 2\}$, as $b^{-}_{m,t}$ and $b^{+}_{m,t}$ respectively. So, on invoking the notations introduced in table 1 and § 5 (*b*), we can write (using β to denote either $+$ or $-$)

$$b^{\beta\times}_{m,t} = \int_{C_t} F_t(C)\, K^{\beta\times}_m(C)\, \mathrm{d}C, \quad t \in \{1 \to 2\}. \tag{7.24}$$

We then find on applying the extinction theorem within $\hat{\Upsilon}_{\mathrm{null}(p)}$, $p \in \{1 \to 2\}$, that the equations equivalent to (7.18) are

$$b^{-\times}_{m,p} + \sum_{n=0}^{M_{tp}} [A^{\times}_{t,p,n,m} b^{+\times}_{n,t} + B^{\times}_{t,p,n,m} b^{+\bar{\times}}_{n,t}] = -a^{\times}_{m,p} \quad (p, t \in \{1, 2\};\ p \neq t), \tag{7.25}$$

where $\mathscr{Z}$ is replaced by $H^{(2)}$ in (7.20) and (7.21). The values of M_{12} and M_{21} depend upon M_1, M_2 and the accuracy to which $F_1(C)$ and $F_2(C)$ are required. We write $F_t(C)$ as

$$F_t(C) = \sigma_t(C) \sum_{q=0}^{M_t} [\alpha^{\mathrm{e}}_{t,q} \Psi^{\mathrm{e}}_{t,q}(C) + \alpha^{\mathrm{o}}_{t,q} \Psi^{\mathrm{o}}_{t,q}(C)] \quad (t \in \{1, 2\}), \tag{7.26}$$

where the $\sigma_t(C)$ are equivalent to the weighting function $\sigma(C)$ introduced in (6.4). The forms of the $\Psi_{t,q}(C)$ are chosen according to the same criteria as are discussed in § 6 (*b*). Substituting (7.26) into (7.24) permits (7.25) to be written as

$$\sum_{q=0}^{M_t} [\alpha^{\mathrm{e}}_{t,q} \Phi^{-\mathrm{e}\times}_{t,m,q} + \alpha^{\mathrm{o}}_{t,q} \Phi^{-\mathrm{o}\times}_{t,m,q}] + \sum_{q=0}^{M_p} [\alpha^{\mathrm{e}}_{p,q} G^{\mathrm{e}\times}_{p,m,q} + \alpha^{\mathrm{o}}_{p,q} G^{\mathrm{o}\times}_{p,m,q}] = -a^{\times}_{m,t} \quad (p, t \in \{1 \to 2\}: p \neq t), \tag{7.27}$$

where there are four different $G_{p,m,q}$:

$$G^{\times\times'}_{p,m,q} = \sum_{n=0}^{M_{pt}} [A^{\times}_{p,t,n,m} \Phi^{\times\times'}_{q,n,q} + B^{\times}_{p,t,n,m} \Phi^{+\times\bar{\times}'}_{p,n,q}] \quad (p, t \in \{1, 2\}; p \neq t; m \in \{0 \to M_p\}; q \in \{0 \to M_t\}), \tag{7.28}$$

where $\mathscr{Z}$ is replaced by $H^{(2)}$ in (7.20) and (7.21). There are eight different $\Phi_{t,m,q}$:

$$\Phi^{\beta\times\times'}_{t,m,q} = \int_{C_t} \sigma_t(C)\, \Psi^{\times}_{t,q}(C)\, K^{\beta\times'}_{m}(C)\, \mathrm{d}C \quad (p, t \in \{1, 2\}; p \neq t; m \in \{0 \to M_{pt}\}; q \in \{0 \to M_t\}). \tag{7.29}$$

Inspection of (7.28) shows that the $G_{p,m,q}$ are got by truncating summations to M_{pt} terms. But it is clear from (7.27) that the accuracy with which each $F_p(C)$ is computed depends upon the relative values of M_p and M_{pt}. This is a manifestation of what is known as the 'relative convergence problem' (Mittra, Itoh & Li 1972). We discuss it further in § 8 (*c*), in so far as it bears on the particular computational examples we have chosen to present: it seems that, at present, each new relative convergence problem has to be treated as a special case.

We find it convenient to denote by $\boldsymbol{\Lambda}_{\alpha,\ldots\omega}$ the matrix with elements $\Lambda_{\alpha,\ldots\omega}$, where α through ω are integer indices. It then follows that (7.20) and (7.21) can be re-expressed as

$$\boldsymbol{A}^{\times}_{t,p,m,n} = \mathbf{cos}\,(m\phi_{tp})\, \boldsymbol{H}^{\times}_{m,n}\, \mathbf{cos}\,(n\phi_{tp}) + \mathbf{sin}\,(m\phi_{tp})\, \boldsymbol{H}^{\bar{\times}}_{m,n}\, \mathbf{sin}\,(n\phi_{tp}), \tag{7.30}$$

$$\boldsymbol{B}^{\times}_{t,p,m,n} = \pm\, \mathbf{sin}\,(m\phi_{tp})\, \boldsymbol{H}^{\times}_{m,n}\, \mathbf{cos}\,(n\phi_{tp}) \mp \mathbf{cos}\,(m\phi_{tp})\, \boldsymbol{H}^{\bar{\times}}_{m,n}\, \mathbf{sin}\,(n\phi_{tp}), \tag{7.31}$$

where the $\mathbf{cos}\,(\cdot)$ and $\mathbf{sin}\,(\cdot)$ matrices are defined to be diagonal, and the elements of the matrices $\boldsymbol{H}^{\times}_{m,n}$ are Howarth & Pavlasek's (1973) 'separation functions':

$$H^{\times}_{m,n} = \tfrac{1}{2}\epsilon_m [H^{(2)}_{m-n}(k\rho_{tp}) \pm H^{(2)}_{m+n}(k\rho_{tp})]. \tag{7.32}$$

Reference to (7.29) and to § 6 (*a*) above shows that $\boldsymbol{\Phi}^{+\times\times'}_{t,m,q}$ is the matrix which has to be inverted to compute the scattering from the tth body when it is isolated, i.e. when the other body is removed. We find it convenient first to evaluate the $\boldsymbol{\Phi}^{+\times\times'}_{t,m,q}$, for t equal to 1 and 2, and then to evaluate the $\boldsymbol{G}_{p,m,q}$ for p equal to 1 and 2. The latter are given by

$$\boldsymbol{G}^{\times\times'}_{p,m,q} = \boldsymbol{A}^{\times}_{p,t,m,n} \boldsymbol{\Phi}^{+\times\times'}_{p,n,q} + \boldsymbol{B}^{\times}_{p,t,n,m} \boldsymbol{\Phi}^{+}_{p,n,q}, \tag{7.33}$$

as (7.27) shows.

A significant computational advantage of our method of ordering the matrix manipulations is that the $\boldsymbol{\Phi}^{\beta\times\times'}_{t,m,q}$ need only be pre-multiplied by rotation matrices if the tth body is rotated about O_t.

8. Applications

The results of a number of numerical solutions to particular direct scattering problems are presented now, in order to demonstrate the computational usefulness of our null field methods. We represent $F(C)$ in terms of the basis functions (6.11) and we employ the substitution (6.6) in (6.10). The factor $\sigma(C)$ in (6.4) is given by (6.8) for sound-soft bodies and is set equal to unity for sound-hard bodies. We restrict the direction (identified by the angle φ), of the incident wave to either 0 or $\frac{1}{2}\pi$, because we find that by so doing we can illustrate all the points we wish to make.

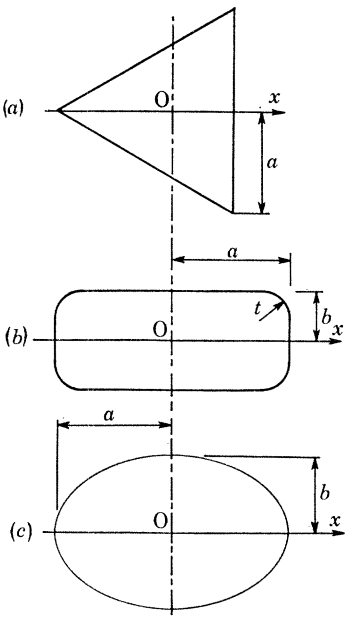

Figure 6. Cylindrical scattering bodies: (*a*) equilateral triangular body; (*b*) rectangular body with corners of variable curvature; (*c*) elliptical body.

This also means that the symmetry existing in all our examples permits us to display the complete behaviour of $F(C)$ by plotting it on only half of C, denoting by $\bar{C}$ the value of C at the point on C where $\phi' = \varphi$ (there is only one such point on each of the bodies we investigate here – refer to figure 6). For convenience, we normalize $F(C)$ such that

$$F(C-\bar{C}) = 1. \tag{8.1}$$

As far as cylindrical bodies are concerned, acoustic diffraction by bodies impenetrable to sound is exactly equivalent to electromagnetic diffraction by perfectly conducting bodies. There is equivalence between sound-soft bodies and electrically polarized fields, and between sound-hard bodies and magnetically polarized fields (cf. Bates 1975*b*). This allows us to compare our results with experimental and computational studies of electromagnetic scattering.

Figure 6 shows the cross-sections of the types of scattering bodies we present results for. We recognize that the forward scattering theorem (cf. Bowman, Senior & Uslenghi 1969, § 1.2.5) is a powerful check on any scattering computation. We use the accuracy to which this theorem is satisfied as an 'energy test' and we introduce the quantity E defined by

$$E = \text{error in energy test.} \tag{8.2}$$

We consider that a computation has 'failed' if $E > 10^{-3}$.

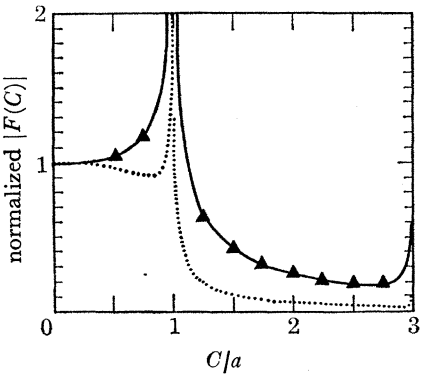

FIGURE 7. Surface source density on a sound-soft triangular cylinder (figure 6(*a*)). ....., $ka = 5.0$; ——, $ka = 1.0$; ▲, measured by Iizuka & Yen (1967) ($ka = 1.0$).

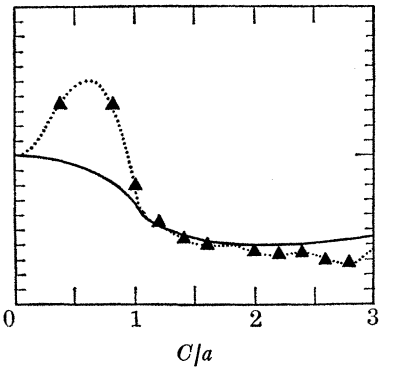

FIGURE 8. Surface source density on a sound-hard triangular cylinder (figure 6(*a*)). ....., $ka = 5.0$; ——, $ka = 1.1$; ▲, calculated by Hunter (1972) ($ka = 5.0$).

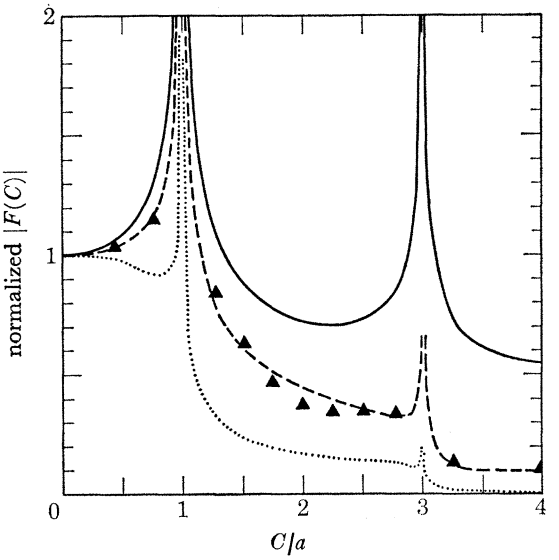

FIGURE 9. Surface source density on a sound-soft square cylinder ($b/a = 1.0$, $t = 0$ in figure 6(*b*)). ....., $ka = 5.0$; – – –, $ka = 1.0$; ——, $ka = 0.1$; ▲, measured by Iizuka & Yen (1967) ($ka = 1.0$).

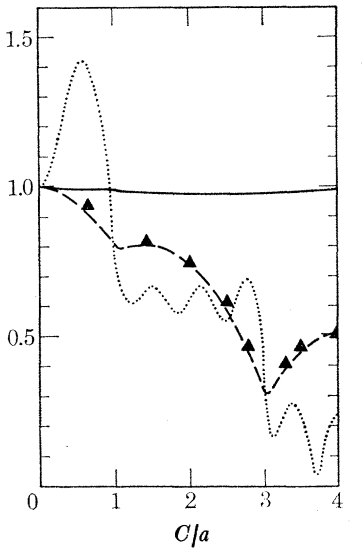

FIGURE 10. Surface source density on a sound-hard square cylinder ($b/a = 1.0$, $t = 0$ in figure 6(*b*)). ....., $ka = 5.0$; – – –, $ka = 1.0$; ——, $ka = 0.1$; ▲, measured by Iizuka & Yen (1967) ($ka = 1.0$).

TABLE 7. VALUES OF M AND C.P.U. TIMES REQUIRED FOR THE CONVERGENT $|F(C)|$ SHOWN IN FIGURES 7 THROUGH 10, $Z = O(1)$ IN EACH CASE

	triangular cross-section				square cross-section $b/a = 1.0$, $t = 0$ in figure 4(*b*)					
	sound-soft		sound-hard		sound-soft			sound-hard		
ka ...	1.0	5.0	1.0	5.0	0.1	1.0	5.0	0.1	1.0	5.0
M	8	15	8	15	5	10	14	5	10	14
c.p.u. time/s	7	9	7	15	6	7	11	6	7	15

(a) *Circular null field method for single scatterers*

Figures 7 through 10 show $|F(C)|$ for some triangular and square bodies. We take $\varphi = 0$. For comparison we reproduce experimental results of Iizuka & Yen (1967) and computational results of Hunter (1972). The computational efficiency of combining Shafai's (1970) transformation with the circular null field method is dramatically emphasized by the low values for M and the large value for Z quoted in table 7.

To illustrate how the circular null field method becomes ill-conditioned as the aspect ratio of the body increases, we show in table 8 how $O(Z)$ and $O(E)$ vary with the elongation of an elliptical sound-soft body.

TABLE 8. CIRCULAR NULL FIELD METHOD APPLIED TO SOUND-SOFT ELLIPTICAL BODY (FIGURE 6 (*c*))

($M = 14$, $ka = 3.14$.)

b/a	1.0	0.8	0.6	0.4	0.2
$O(Z)$	10^{0}	10^{-1}	10^{-4}	10^{-8}	10^{-12}
$O(E)$	10^{-9}	10^{-7}	10^{-6}	10^{-3}	fail

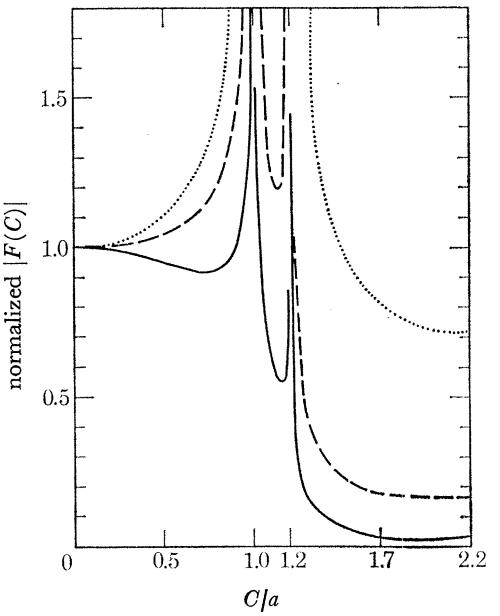

FIGURE 11. Surface source density on a sound-soft rectangular cylinder ($b/a = 0.1$, $t = 0$ in figure 6 (*b*)). ——, $ka = 3.14$, $M = 14$, c.p.u. time = 22 s; – – –, $ka = 1.0$, $M = 10$, c.p.u. time = 20 s; ……, $ka = 0.1$, $M = 4$, c.p.u. time = 15 s.

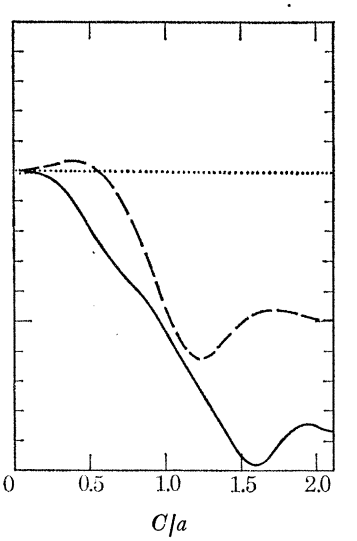

FIGURE 12. Surface source density on a sound-hard rectangular cylinder ($b/a = 0.1$, $t = a$ in figure 6 (*b*)). ——, $ka = 3.14$, $M = 10$, c.p.u. time = 62 s; – – –, $ka = 1.0$, $M = 6$, c.p.u. time = 32 s; ……, $ka = 0.1$, $M = 4$, c.p.u. time = 20 s.

(b) *Elliptic null field method for single scatterers*

Figures 11 and 12 show $|F(C)|$ for an elongated rectangular body with rounded corners. We take $\varphi = \pi/2$. To obtain these results the semi-focal distance d of the elliptic cylinder coordinates is taken as $\check{d}$, where

$$\check{d} = \{1 - (b/a)^2\}^{\frac{1}{2}} a, \tag{8.3}$$

which makes Ω_{null} as large a part of Ω_- as possible. If $d/\check{d}$ is reduced to zero, the elliptic null field method becomes the circular null field method and the part of Ω_- spanned by Ω_{null} is decreased. Accuracy of numerical integration is crucial for the success of null field methods. We denote by L_0 the factor by which the number of ordinates, used when the extended Simpson rule is employed to evaluate (6.10), has to be increased, in order to obtain solutions from (6.9) for the α_q to the required accuracy, when the semi-focal distance of the elliptic cylinder coordinates is changed from $\check{d}$ to some other value. Table 9 shows the marked increase and decrease of Z and L_0, respectively, as d is increased from zero to $\check{d}$, for a sound-soft rectangular cylinder.

TABLE 9. ELLIPTIC NULL FIELD METHOD APPLIED TO SOUND-SOFT RECTANGULAR CYLINDER (SEE FIGURE 6(*b*): $b/a = 0.1$, $t = 0$)

$d/\check{d}$ ...	0	0.25	0.5	0.75	1.0
	$ka = 1.0$, $M = 10$				
O(Z)	10^{-10}	10^{-4}	10^{-4}	10^{-2}	10^{0}
L_0	> 8	8	4	2	1
	$ka = 3.14$, $M = 14$				
O(Z)	10^{-20}	10^{-11}	10^{-9}	10^{-5},	10^{-9}
L_0	> 4	> 4	> 4	4	1

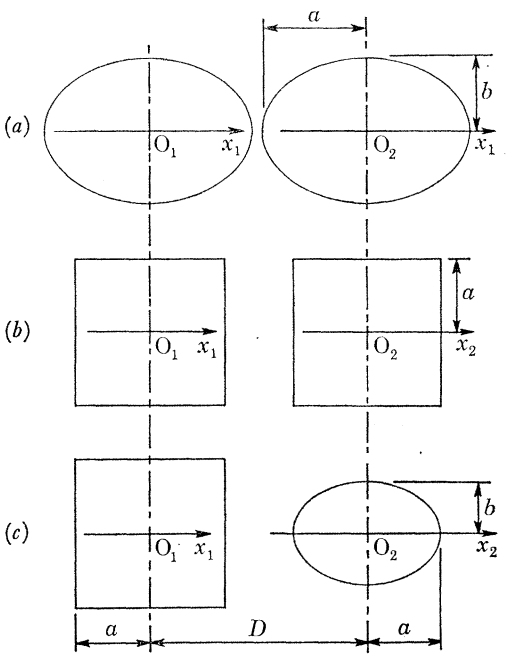

FIGURE 13. Pairs of cylindrical scattering bodies: (*a*) two identical elliptic cylinders; (*b*) two identical square cylinders; (*c*) an elliptic cylinder and a square cylinder.

(*c*) *Circular null field method for pairs of bodies*

We take ψ_0 to be a plane wave incident at an angle corresponding to $\phi_1 = \varphi$. We denote by $\bar{C}_t$ the value of C_t at the point where $\phi_t' = \varphi$. There is only one such point on each of the bodies examined here (refer to figure 13).

Our purpose is to demonstrate the computational convenience of our method, and we simplify the examples as much as is consistent with this. We make both bodies about the same size, so that we can take

$$M_1 = M_2 = M; \quad M_{12} = M_{21} = N, \tag{8.4}$$

where the integers M and N are introduced for convenience.

Figure 13 shows the three pairs of bodies we investigate. Their symmetry ensures that

$$\boldsymbol{\Phi}^{\beta\mathrm{eo}}_{t,m,q} = \boldsymbol{\Phi}^{\beta\mathrm{oe}}_{t,m,q} = 0; \tag{8.5}$$

$$\boldsymbol{\Phi}^{\beta\mathrm{ee}}_{t,m,q} = \boldsymbol{\Phi}^{\beta\mathrm{oo}}_{t,m,q} = 0 \quad \text{for } (m+q) \text{ odd}; \tag{8.6}$$

$$\boldsymbol{A}^{\times}_{t,p,m,n} = \boldsymbol{H}^{\times}_{m,n}; \tag{8.7}$$

$$\boldsymbol{B}_{t,p,m,n} = 0, \tag{8.8}$$

which have the effect of significantly reducing the required computational effort. The coefficients of the multipole expansions of ψ_0 are then

$$a^{\times}_{m,1} = 4\mathrm{i}^{m+1}\,\mathrm{sc}\,(m\varphi); \tag{8.9}$$

$$a^{\times}_{m,2} = 4\mathrm{i}^{m+1}\exp\left(\mathrm{i}k\rho_{12}\cos\left(\phi_{12}-\varphi\right)\mathrm{sc}\,(m\varphi)\right). \tag{8.10}$$

TABLE 10. NUMERICAL CONVERGENCE OF THE FIRST SIX $\alpha^{\mathrm{e}}_{1,q}$ AND $\alpha^{\mathrm{e}}_{2,q}$ FOR THE PAIR OF SOUND-HARD ELLIPTICAL CYLINDERS SHOWN IN FIGURE 13(*a*) WITH $b/a = 0.76$, $ka = 1.54$, $kD = 4.0$, $\varphi = 0$ (hence $\alpha^{\mathrm{o}}_{t,q} = 0$; $t \in \{1 \to 2\}$), $N = 23$

(In each entry in the table, the real part of $\alpha_{t,q}$ is above the imaginary part of $\alpha_{t,q}$.)

	q	$M = 4$	$M = 6$	$M = 8$	$M = 10$
$\alpha^{\mathrm{e}}_{1,q}$	0	−0.097966	−0.097733	−0.097749	−0.097749
		−0.037092	−0.037752	−0.037772	−0.037772
	1	−0.132527	−0.130935	−0.130979	−0.130981
		−0.175235	−0.175666	−0.175697	−0.175698
	2	0.112851	0.106871	0.106819	0.106810
		−0.056340	−0.056320	−0.056476	−0.056485
	3	−0.006684	−0.006905	−0.006946	−0.006949
		0.030580	0.028691	0.028624	0.028618
	4	—	−0.011436	−0.011489	−0.011513
		—	−0.003294	−0.003658	−0.003689
	5	—	−0.000700	−0.000805	−0.000817
		—	−0.002774	−0.002905	−0.002921
$\alpha^{\mathrm{e}}_{2,q}$	0	−0.044558	−0.044673	−0.044679	−0.044699
		0.103017	0.103800	0.103780	0.103779
	1	−0.092042	−0.090970	−0.090919	−0.090914
		0.195611	0.195603	0.195641	0.195643
	2	−0.158362	−0.152364	−0.152362	−0.152383
		−0.167660	−0.165631	−0.165746	−0.165752
	3	0.024354	0.023350	0.023336	0.023336
		−0.020391	−0.019466	−0.019436	−0.019432
	4	—	0.010720	0.010766	0.010777
		—	0.006534	0.006334	0.006326
	5	—	−0.001900	−0.001946	−0.001951
		—	0.001172	0.001194	0.001199

TABLE 11. NUMERICAL CONVERGENCE OF THE FIRST SEVEN $\alpha^{e}_{1,q}$, $\alpha^{o}_{1,q}$ FOR THE PAIR OF SOUND-SOFT SQUARE CYLINDERS SHOWN IN FIGURE 13(*b*), WITH $ka = 3.14$, $kD = 10.0$, $\varphi = \frac{1}{2}\pi$ (hence $\alpha_{1,q} = \alpha_{2,q}$), $M = 13$

(In each entry in the table, the real part of $\alpha_{1,q}$ is above the imaginary part of $\alpha_{1,q}$. The relative convergence test is satisfied when $N = 30$.)

	$\alpha^{e}_{1,q}$			$\alpha^{o}_{1,q}$		
q	$N = 12$	$N = 15$	$N = 35$	$N = 12$	$N = 15$	$N = 35$
0	−0.250245	−0.249979	−0.249982	—	—	—
	0.028165	0.028227	0.028229	—	—	—
1	0.506148	0.506562	0.506557	−0.920619	−0.920548	−0.92049
	−0.140652	−0.140831	−0.140828	0.358002	0.358060	0.358061
2	1.25160	1.25197	1.25197	−0.011035	−0.010970	−0.010970
	−0.070592	−0.070763	−0.070758	0.324950	0.324982	0.324984
3	0.388148	0.388433	0.388434	0.401695	0.401757	0.401752
	0.005621	0.005526	0.005531	0.682449	0.682520	0.682521
4	0.309475	0.309167	0.309168	−0.228484	−0.228379	−0.228382
	−0.213278	−0.213499	−0.213497	0.308493	0.308160	0.308159
5	0.143397	0.143382	0.143385	−0.035410	−0.035569	−0.035570
	0.114938	0.114824	0.114825	0.221693	0.221711	0.221713
6	0.142208	0.142189	0.142190	−0.103601	−0.103596	−0.103594
	−0.089844	−0.089845	−0.089843	0.001584	0.001563	0.001553

TABLE 12. NUMERICAL CONVERGENCE OF THE FIRST SEVEN $\alpha^{e}_{1,q}$, $\alpha^{o}_{1,q}$ FOR THE PAIR OF SOUND-SOFT SQUARE CYLINDERS SHOWN IN FIGURE 13(*b*), WITH $ka = 3.14$, $kD = 7.61$, $\varphi = \frac{1}{2}\pi$ (hence, $\alpha_{1,q} = \alpha_{2,q}$), $M = 13$

(In each entry in the table, the real part of $\alpha_{1,q}$ is above the imaginary part of $\alpha_{1,q}$. The relative convergence test is satisfied when $N = 42$.)

	$\alpha^{e}_{1,k}$			$\alpha^{o}_{1,q}$		
q	$N = 20$	$N = 35$	$N = 42$	$N = 20$	$N = 35$	$N = 42$
0	−0.563418	−0.561913	−0.561905	—	—	—
	0.064934	0.068325	0.068494	—	—	—
1	−0.085861	−0.087844	−0.087960	−1.00278	−1.00179	−1.00178
	−0.066684	−0.064534	−0.064478	0.109593	0.105853	0.105858
2	0.743689	0.739456	0.739450	−0.113282	−0.111922	−0.111914
	−0.003804	−0.00392	−0.003981	−0.112723	−0.115332	−0.115322
3	−0.008291	−0.014434	−0.014574	0.394478	0.391873	0.391866
	0.067807	0.066239	0.066106	0.153272	0.152979	0.152971
4	0.016540	0.009097	0.008741	−0.067097	−0.080693	−0.080764
	−0.160202	−0.160763	−0.160885	−0.126332	−0.122468	−0.122532
5	−0.073251	−0.066012	−0.065872	0.134041	0.137440	0.137432
	0.145867	0.145084	0.145141	0.044496	0.045850	0.045853
6	0.009671	0.019729	0.019898	−0.067366	−0.057729	−0.057725
	−0.076490	−0.078301	−0.078249	−0.026791	−0.028713	−0.028694

TABLE 13. ENERGY TEST FOR THE PAIR OF CYLINDERS TO WHICH TABLE 12 REFERS

M	3	4	5	6	8	10
E	-0.51×10^{-2}	0.19×10^{-2}	-0.56×10^{-3}	-0.28×10^{-4}	0.13×10^{-5}	0.27×10^{-6}

We denote the value of $|G_{t,m,q}|$, evaluated when N has a particular value, by $|G_{t,m,q}|_N$. We denote the value of $\alpha_{t,q}$, evaluated when M has a particular value, by $\alpha_{t,q)M}$. The elegant approach of Mittra *et al.* (1972) to relative convergence is impracticable for us, but we find the following 'relative convergence test' effective. We require $|\alpha_{t,q)M}|$ to differ by less than some desired amount from both $|\alpha_{t,q)M-1}|$ and $|\alpha_{t,q)M-2}|$ while demanding that N is large enough to ensure that each $|G_{t,m,q}|_N$ differs by less than one part in 10^γ from both $|G_{t,m,q}|_{N-1}$ and $|G_{t,m,q}|_{N-2}$. Tables 10 through 12 confirm that we obtain manifest numerical convergence by this procedure when $\gamma = 3$. We can increase our confidence in the results by applying the energy test. Table 13

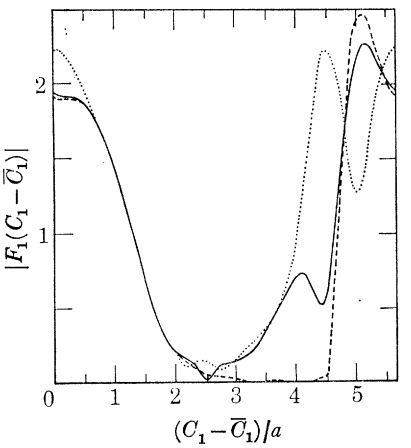

FIGURE 14. Surface source density on cylinder 1, for two sound-soft elliptic cylinders ($ka = 3.14$, $b/a = 0.8$ in figure 13 (*a*)). – – –, $kD = 6.28$ (contact), $M = 13$, $N = 25$; ——, $kD = 12.57$, $M = 13$, $N = 20$; ....., $kD = 15.72$, $M = 13$, $N = 15$.

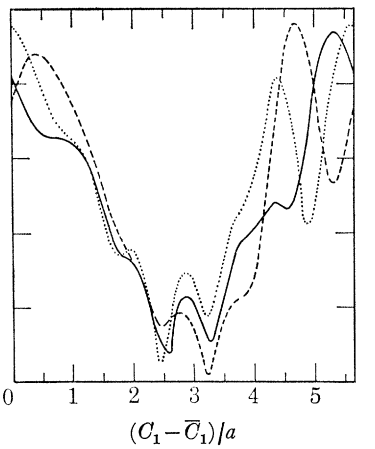

FIGURE 15. Surface source density on cylinder 1, for two sound-hard elliptic cylinders ($ka = 3.14$, $b/a = 0.8$ in figure 13 (*a*)). ....., $kD = 7.5$, $M = 13$, $N = 25$; ——, $kD = 9.43$, $M = 13$, $N = 22$; – – –, $kD = 12.57$, $M = 13$, $N = 20$.

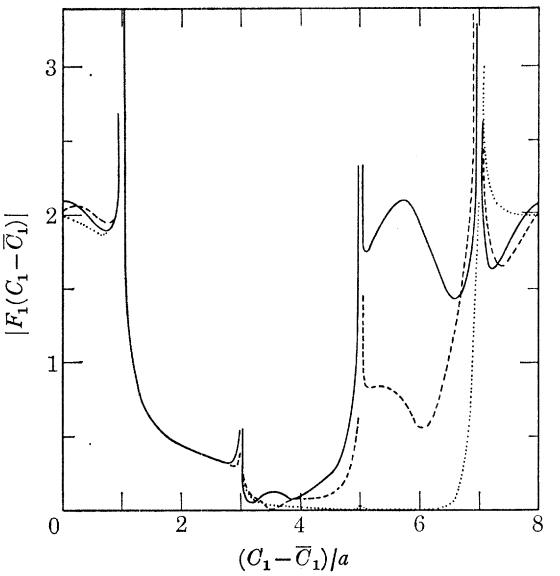

FIGURE 16. Surface source density on cylinder 1, for two sound-soft square cylinders ($ka = 3.14$ in figure 13 (*b*)). ....., $kD = 7.61$, $M = 13$, $N = 42$; ——, $kD = 10.0$, $M = 13$, $N = 30$; – – –, $kD = 12.57$, $M = 13$, $N = 25$.

indicates the variation of E with M for the pair of cylinders to which table 10 refers. The energy test is successful for M as small as 5, which might be thought remarkable when recalling the slow convergence of some previously reported methods (quoted in § 1).

Figures 14 through 18 display the magnitudes of the surface source densities, plotted against $C_t - \bar{C}_t$, for the three types of pairs of cylinders shown in figure 13, when ψ_0 is incident at an angle $\varphi = \frac{1}{2}\pi$. This means that the symmetry existing in our examples involving identical cylinders (cf. figure 13*a*, *b*) permits us to display the complete behaviour to F_1 and F_2 by plotting F for just one cylinder, as we do in figures 14 through 16. Multiple resonances of the kind discussed by Howarth (1973) are clearly indicated. These resonances are due to the field reflected from one body onto the other being in places more intense than the incident field.

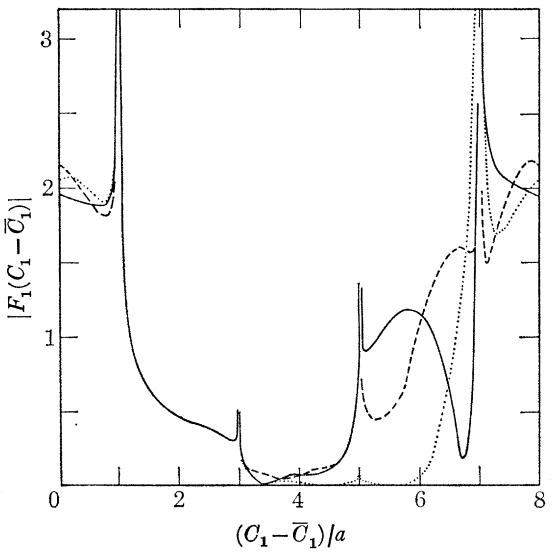

FIGURE 17. Surface source density on cylinder 1, for two sound-soft cylinders: a square cylinder (cylinder 1) and an elliptic cylinder ($ka = 3.14$, $b/a = 0.8$ in figure 13 (*c*)). ....., $kD = 7.61$, $M = 13$, $N = 42$; ——, $kD = 11.5$, $M = 13$, $N = 30$; – – –, $kD = 15.72$, $M = 13$, $N = 25$.

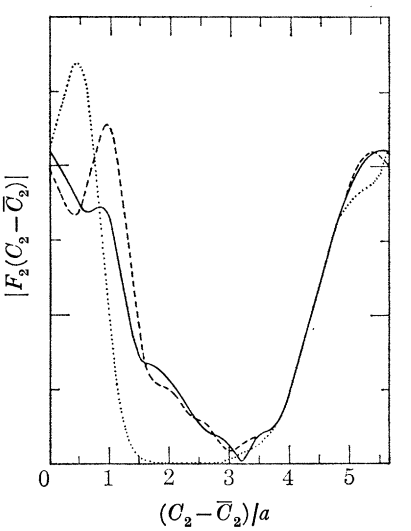

FIGURE 18. Surface source density on cylinder 2, for two sound-soft cylinders: a square cylinder and an elliptic cylinder (cylinder 2) ($ka = 3.14$, $b/a = 0.8$ in figure 13 (*c*)). ....., $kD = 7.61$, $M = 13$, $N = 42$; ——, $kD = 11.5$, $M = 13$, $N = 30$; – – –, $kD = 15.72$, $M = 13$, $N = 25$.

Reference to figure 13 (*a*) and (*b*) shows that the value of ρ_t on $\hat{\Gamma}_{+t}$ (refer to § 7 and figure 5) for the square cylinders is greater than the value for the elliptic cylinders. This shows up in the increased values of N for the square cylinder compared with the elliptic cylinder (see captions to figures 15 and 16), required to satisfy the relative convergence test. Reference to figure 13 (*b*) also shows that when the square cylinders are so close that $D < 2.41a$ then Γ_{+1} and Γ_{+2} intersect C_2 and C_1 respectively (refer to figure 3), which means that the sizes of $\hat{\Omega}_{\text{null}(1)}$ and $\hat{\Omega}_{\text{null}(2)}$ are reduced. Examination of tables 3 and 4 shows that the $\alpha_{t,q}$ are increasingly sensitive in their higher significant figures to N as D decreases. As $\hat{\Omega}_{\text{null}(1)}$ and $\hat{\Omega}_{\text{null}(2)}$ are progressively reduced γ must be increased to maintain the same accuracy in the $\alpha_{t,q}$. There is no corresponding reduction in the sizes of $\hat{\Omega}_{\text{null}(1)}$ and $\hat{\Omega}_{\text{null}(2)}$ when the elliptic cylinders of figure 13 (*a*) touch, so that $\gamma = 3$ is sufficient to maintain the accuracy of the $\alpha_{t,q}$.

The c.p.u. time needed to compute the matrices $\Phi^{\beta\times\times'}_{t,m,q}$ – for the elliptical and square cylinders to which figures 14 through 18 apply – was 6 s and 13 s respectively (with $M = 13$ and $N = 35$).

The additional c.p.u. time required to compute the surface source densities shown in figures 14 through 18 was close to 14 s in each case. Only about 0.2 s was needed to compute the matrices $A_{t,p,m,n}$.

9. Conclusions

The results presented in § 8 (*a*), (*b*) support our contention that the elliptic null field method can handle bodies of large aspect ratio. The essential thing is to choose the parameters of the elliptic cylinder coordinates such that Ω_{null} occupies as much of Ω_- as possible. When this is done the numerical stability and accuracy of the solutions seem to be virtually independent of aspect ratio, and yet the orders of the matrices which must be inverted are as small as those previously reported in studies of bodies of small aspect ratio by the circular and spherical null field methods (cf. Ng & Bates 1972; Bates & Wong 1974). We point out that our approach is a generalized systematic procedure of the sort which Jones (1974*a*), who examines the work of Schenck (1968) and Ursell (1973), suggests should be derivable from the extended boundary condition.

A notable aspect of the null field approach to multiple scattering is that it permits multipole expansions to be applied conveniently to bodies of arbitrary shape. The results presented in § 8 (*c*) confirm that the scattering from interacting bodies having different shapes can be computed to useful accuracy by inverting matrices whose orders are low, by comparison with what has been reported before. Another significant aspect of these results is that they demonstrate that the null field method permits near fields to be calculated expeditiously to useful accuracies.

A serious theoretical shortcoming of our method is that neither the uniqueness nor the convergence of the numerical solutions has been rigorously demonstrated. But we have the following strong theoretical reason for confidence in our procedures. The sources quoted in § 6 (*a*) show rigorously that $\tilde{f}_L$, as defined by (6.1), converges uniquely in a mean square sense to the solution f of (4.2). All our computational experience suggests that the apparent numerical convergence to of $\hat{f}_L$, as defined by (6.3) with the $\hat{\Psi}_{j,l}$ possessing the characteristics set down in § 6 (*a*) (note also the more extensive discussion of the Ψ_m in § 6 (*b*)), is much faster than the apparent numerical convergence of $\tilde{f}_L$ to f. So we feel justified in hypothesizing that $\hat{f}_L$ converges uniquely to f, in a mean square sense at least. But we offer as a challenge to numerical analysts this convergence and uniqueness question, together with the more important problem of devising accurate *a priori* measures of the rate of convergence of numerical solutions to integral equations. The latter are needed so that the accuracy of a solution for a single value of L, or M, can be usefully assessed without having to make further (usually expensive) calculations for several slightly larger values of L, or M.

The results reported here for totally reflecting bodies of arbitrary shape, together with Peterson and Ström's work on penetrable bodies of restricted shape, contribute towards making Waterman's approach globally efficient computationally.

We thank our colleague Dr A. W. McInnes, also Professor W. M. Boerner of the University of Manitoba, for several useful discussions. One of us, D. J. N. Wall, acknowledges the support of a New Zealand University Grants Committee Postgraduate Scholarship.

PHILOSOPHICAL TRANSACTIONS OF THE ROYAL SOCIETY A MATHEMATICAL, PHYSICAL & ENGINEERING SCIENCES

References

Abeyaskere, W. D. M. 1972 An introduction to the algorithmic Albert–Synge antenna equation. *Proc. IREE* (Australia) **33**, 90–97.

Abramowitz, M. & Stegun, I. A. 1968 *Handbook of mathematical functions*. New York: Dover.

Ahluwalia, H. P. S. & Boerner, W. M. 1974 Application of a set of e.m. inverse boundary conditions to the profile characteristics inversion of imperfectly conducting spherical shapes. *IEEE Trans. Antennas Propag.* AP-**22**, 673–682.

Al-Badwaihy, K. A. & Yen, J. L. 1974 Hemispherically capped thick cylindrical monopole with a conical feed section. *IEEE Trans. Antennas Propag.* AP-**22**, 477–481.

Al-Badwaihy, K. A. & Yen, J. L. 1975 Extended boundary condition integral equations for perfectly conducting and dielectric bodies: formulation and uniqueness. *IEEE Trans. Antennas Propag.* AP-**2**, 546–551.

Albert, G. E. & Synge, J. L. 1948 The general problem of antenna radiation and the fundamental integral equation with application to an antenna of revolution – Part 1. *Q. appl. Math.* **6**, 117–131.

Avetisyan, A. A. 1970 A generalized method of separation of variables and diffraction of electromagnetic waves of bodies of revolution. *Radio Engng Electron. Phys.* **15**, 1–9.

Bates, R. H. T. 1968 Modal expansions for electromagnetic scattering from perfectly conducting cylinders of arbitrary cross-section. *Proc. IEE* **115**, 1443–1445.

Bates, R. H. T. 1969 The theory of the point-matching method for perfectly conducting waveguides and transmission lines. *IEEE Trans. Microwave Theory Tech.* MTT-**17**, 294–301.

Bates, R. H. T. 1975*a* New justification for physical optics and the aperture-field method. *Proc. XXth AGARD Meeting on Electromagnetic Wave Propagation Involving Irregular Surfaces and Inhomogeneous Media*, The Hague, Netherlands; AGARD Conf. Publication no. CPP-144, 36-1 to 36-7.

Bates, R. H. T. 1975*b* Analytic constraints on electromagnetic field computations. *IEEE Trans. Microwave Theory Tech.* MTT-**23**, 605–623.

Bates, R. H. T. & Ng, F. L. 1972 Polarization-source formulation of electromagnetism and dielectric-loaded waveguides. *Proc. IEE* **119**, 1568–1574.

Bates, R. H. T. & Ng, F. L. 1973 Point matching computation of transverse resonances. *Int. J. numerical Methods Engng* **6**, 155–168.

Bates, R. H. T. & Wong, C. T. 1974 The extended boundary condition and thick axially symmetric antennas. *Appl. Sci. Res.* **29**, 19–43.

Bickley, W. G. 1929 Two-dimensional potential problems concerning a single closed boundary. *Phil. Trans. R. Soc. Lond.* A **228**, 235–274.

Bickley, W. G. 1934 Two-dimensional potential problems for the space outside a rectangle. *Proc. Lond. math. Soc.* **37**, 82–105.

Blanch, G. 1964 Numerical evaluation of continued fractions. *SIAM Rev.* **6**, 383–421.

Blanch, G. 1966 Numerical aspects of Mathieu eigenvalues. *Rend. Circ. Mat. Palermo* **2**, 51–97.

Bolomey, J. C. & Tabbara, W. 1973 Numerical aspects on coupling between complementary boundary value problems. *IEEE Trans. Antennas Propag.* AP-**21**, 356–363.

Bolomey, J. C. & Wirgin, A. 1974 Numerical comparison of the Green's function and the Waterman and Rayleigh theories of scattering from a cylinder with arbitrary cross section. *Proc. IEE* **121**, 794–804.

Born, M. & Wolf, E. 1970 *Principles of optics*, 4th edn. Oxford: Pergamon.

Bowman, J. J., Senior, T. B. A. & Uslenghi, P. L. E. 1969 *Electromagnetic and acoustic scattering by simple shapes*. Amsterdam: North-Holland.

Burke, J. E. & Twersky, V. 1964 On scattering of waves by many bodies. *J. Res. natn. Bur. Stand.* **68**D, 500–510.

Cheng, S. L. 1969 Multiple scattering of elastic waves by parallel cylinders. *J. appl. Mech.* **36**, 523–527.

Conte, S. D. 1965 *Elementary numerical analysis*. New York: McGraw-Hill.

Copley, L. G. 1967 Integral equation method for radiation from vibrating bodies. *J. Acoust. Soc. Am.* **41**, 807–816.

Cruzan, O. R. 1962 Translational addition theorems for spherical vector wave functions. *Q. Appl. Math.* **20**, 33–40.

De Goede, J. & Mazur, P. 1972 On the extinction theorem in electrodynamics. *Physica* **58**, 568–584.

Ewald, P. P. 1916 *Ann. Phys.* **49**, 1.

Fenlon, F. H. 1969 Calculation of the acoustic radiation field at the surface of a finite cylinder by the method of weighted residuals. *Proc. IEEE* **57**, 291–306.

Flammer, C. 1957 *Spheroidal wave functions*. California: Stanford University Press.

Gavorun, N. N. 1959 *Dokl. Akad. Nauk. SSSR.* **126**, 49–52.

Gavorun, N. N. 1961 The numerical solution of an integral equation of the first kind for the current density in an antenna body of revolution. *Zh. Vych. Mat.* **1**, 664–679.

Green, C. D. 1969 *Integral equation methods*. London: Nelson.

Harrington, R. F. 1968 *Field computation by moment methods*. New York: Macmillan.

Hessel, A. & Oliner, A. A. 1965 A new theory of Wood's anomalies on optical gratings. *Appl. Opt.* **4**, 1275–1297.

Hizal, A. & Marincic, A. 1970 New rigorous formulation of electromagnetic scattering from perfectly conducting bodies of arbitrary shape. *Proc. IEE* **117**, 1639–1647.

PHILOSOPHICAL TRANSACTIONS OF THE ROYAL SOCIETY A MATHEMATICAL, PHYSICAL & ENGINEERING SCIENCES

Hönl, H., Maue, A. W. & Westpfahl, K. 1961 In Flügge, S. (Ed.), *Handbuch der Physik* **25/1**. Berlin: Springer-Verlag.

Howarth, B. A. 1973 Multiple scattering resonances between parallel conducting cylinders. *Can. J. Phys.* **51**, 2415–2427.

Howarth, B. A. & Pavlasek, T. J. F. 1973 Multipole induction: a novel formulation of multiple scattering of scalar waves. *J. appl. Phys.* **44**, 1162–1167.

Howarth, B. A., Pavlasek, T. J. F. & Silvester, P. 1974 A graphical representation for interpreting scalar wave multiple-scattering phenomena. *J. comp. Phys.* **15**, 266–285.

Hunter, J. D. 1972 The surface current density on perfectly conducting polygonal cylinders. *Can. J. Phys.* **50**, 139–150.

Hunter, J. D. 1974 Scattering by notched and wedged circular cylinders. *Int. J. Electron.* **36**, 375–381.

Hunter, J. D. & Bates, R. H. T. 1972 Secondary diffraction from close edges on perfectly conducting bodies. *Int. J. Electron.* **32**, 321–333.

Iizuka, K. & Yen, J. L. 1967 Surface currents on triangular and square metal cylinders. *IEEE Trans. Antennas Propag.* AP-**15**, 795–801.

Jones, D. S. 1964 *The theory of electromagnetism.* Oxford: Pergamon.

Jones, D. S. 1974*a* Integral equations for the exterior acoustic problem. *Q. Jl Mech. appl. Math.* **27**, 129–142.

Jones, D. S. 1974*b* Numerical methods for antenna problems. *Proc. IEE* **121**, 573–582.

Kantorovich, L. V. & Krylov, V. I. 1958 *Approximate methods of higher analysis.* Netherlands: P. Noordhoff.

Karp, S. N. & Zitron, N. R. 1961*a* Higher-order approximations in multiple scattering: I. Two-dimensional case. *J. math. Phys.* **2**, 394–402.

Karp, S. N. & Zitron, N. R. 1961*b* Higher-order approximations in multiple scattering. II. Three-dimensional case *J. math. Phys.* **2**, 402–406.

King, B. J. & Van Buren, A. L. 1973 A general addition theorem for spheroidal wave functions. *SIAM J. Math. Anal.* **4**, 149–160.

Lewin, L. 1970 On the restricted validity of point-matching techniques. *IEEE Trans. Microwave Theory Tech.* MTT-**18**, 1041–1047.

Liang, C. & Lo, Y. T. 1967 Scattering by two spheres. *Radio Sci.* **2** (N.S.), 1481–1495.

Love, A. E. H. 1901 The integration of the equations of propagation of electric waves. *Phil. Trans. R. Soc. Lond.* A **197**, 1–45.

Meixner, J. & Schäfke, F. W. 1954 *Mathieusche Funktionen und Sphäroidfunktionen.* Berlin: Springer-Verlag.

Mittra, R., Itoh, T. & Li, T. 1972 Analytical and numerical studies of the relative convergence phenomenon arising in the solution of an integral equation by the moment method. *IEEE Trans. Microwave Theory Tech.* MTT-**20**, 96–104.

Morse, P. M. & Feshbach, H. 1953 *Methods of theoretical physics.* New York: McGraw-Hill.

Morse, P. M. & Ingard, K. U. 1968 *Theoretical acoustics.* New York: MCraw-Hill.

Ng, F. L. & Bates, R. H. T. 1972 Null field method for waveguides of arbitrary cross section. *IEEE Trans. Microwave Theory Tech.* MTT-**20**, 658–662.

Olaofe, G. O. 1970 Scattering by two cylinders. *Radio Sci.* **5**, 1351–1360.

Oseen, C. W. 1915 *Ann. Phys.* **48**, 1.

Pattanayak, D. N. & Wolf, E. 1972 General form and a new interpretation of the Ewald–Oseen extinction theorem. *Opt. Commun.* **6**, 217–220.

Peterson, B. & Ström, S. 1974 T-matrix formulation of electromagnetic scattering. *Phys. Rev.* D **10**, 2670–2690.

Pogorzelski, W. 1966 *Integral equations and their applications.* Oxford: Pergamon.

Rayleigh, Lord 1892 On the influence of obstacles arranged in rectangular order upon the properties of a medium. *Phil. Mag.* **34**, 481. In *Collected works*, vol. 4, 1903. Cambridge University Press.

Row, R. V. 1955 Theoretical and experimental study of electromagnetic scattering by two identical conducting cylinders. *J. appl. Phys.* **26**, 666–675.

Sack, R. A. 1964 Three-dimensional addition theorem for arbitrary functions involving expansions in spherical harmonics. *J. math. Phys.* **5**, 252–259.

Saermark, K. 1959 Scattering of a plane monochromatic wave by a system of strips. *Appl. Sci. Res.* B-**7**, 417–440.

Schenck, H. A. 1968 Improved integral formulation for acoustic radiation problems. *J. Acoust. Soc. Am.* **44**, 41–58.

Sein, J. J. 1970 A note on the Ewald–Oseen extinction theorem. *Opt. Commun.* **2**, 170–172.

Sein, J. J. 1975 General extinction theorems. *Opt. Commun.* **14**, 157–160.

Shafai, L. 1970 An improved integral equation for the numerical solution of two-dimensional diffraction problems. *Can. J. Phys.* **48**, 954–963.

Silver, S. 1965 *Microwave antenna theory and design.* New York: Dover.

Smithies, F. 1958 *Integral equations.* Cambridge University Press.

Stein, S. 1961 Addition theorems for spherical wave functions. *Q. appl. Math.* **19**, 15–24.

Synge, J. L. 1948 The general problems of antenna radiation and the fundamental integral equation with application to an antenna of revolution – Part II. *Q. appl. Math.* **6**, 133–156.

PHILOSOPHICAL TRANSACTIONS OF THE ROYAL SOCIETY A MATHEMATICAL, PHYSICAL & ENGINEERING SCIENCES

Taylor, C. D. & Wilton, D. R. 1972 The extended boundary condition solution of the dipole antenna of revolution. *IEEE Trans. Antennas Propag.* AP-**20**, 772–776.
Twersky, V. 1960 On multiple scattering of waves. *J. Res. natn Bur. Stand.* **64**D, 715–730.
Twersky, V. 1962*a* In *Electromagnetic waves* (ed. R. E. Langer). Wisconsin: University of Wisconsin Press.
Twersky, V. 1962*b* Multiple scattering by arbitrary configurations in three dimensions. *J. math. Phys.* **3**, 83–91.
Twersky, V. 1967 Multiple scattering of electromagnetic waves by arbitrary configurations. *J. math. Phys.* **8**, 589–610.
Ursell, F. J. 1973 On the exterior problem of acoustics. *Proc. Camb. Phil. Soc.* **74**, 117–125.
Vasil'ev, E. N. 1959 Excitation of a smooth perfectly conducting solid of revolution – I and II. *Iz. VUZ Radiofizika* **2**, 588–601.
Vasil'ev, E. N., Malushkov, G. D. & Falunin, A. A. 1967 Integral equations of the first kind in some problems of electrodynamics. *Soviet Phys. tech. Phys.* **12**, 303–310.
Vasil'ev, E. N. & Seregina, A. R. 1963 The excitation of a thick cylinder of finite length. *Radiotekh. Electron.* **8**, 1972–1979.
Waterman, P. C. 1965 Matrix formulation of electromagnetic scattering. *Proc. IEEE* **53**, 805–812.
Waterman, P. C. 1969*a* Scattering by dielectric obstacles. *Alta Frequenza* **38**(Speciale), 348–352.
Waterman, P. C. 1969*b* New formulation of acoustic scattering. *J. Acoust. Soc. Am.* **45**, 1417–1429.
Waterman, P. C. 1971 Symmetry, unitarity and geometry in electromagnetic scattering. *Phys. Rev.* D. **3**, 825–839.
Waterman, P. C. 1975 Scattering by periodic surfaces. *J. Acoust. Soc. Am.* **57**, 791–802.
Watson, G. N. 1966 *A treatise on the theory of Bessel functions*, 2nd edn. Cambridge University Press.
Wirgin, A. 1975 Resonance scattering from an arbitrarily shaped protuberance on a ground plane. *Opt. Acta* **22**, 47–58.
Zabreyko, P. P., Koshelev, M. A., Mikhin, S. G., Rakovshchik, L. S. & Stet'senko, V. Ya. 1975 *Integral equations – a reference text.* Leyden: Noordhoff.
Zaviska, F. 1913 Über die Beugung elektromagnetischer Wellen an paralleln undendlich langen Kreiszylindern. *Ann. Phys.* **40**, 1023.

PHILOSOPHICAL TRANSACTIONS OF THE ROYAL SOCIETY A MATHEMATICAL, PHYSICAL & ENGINEERING SCIENCES